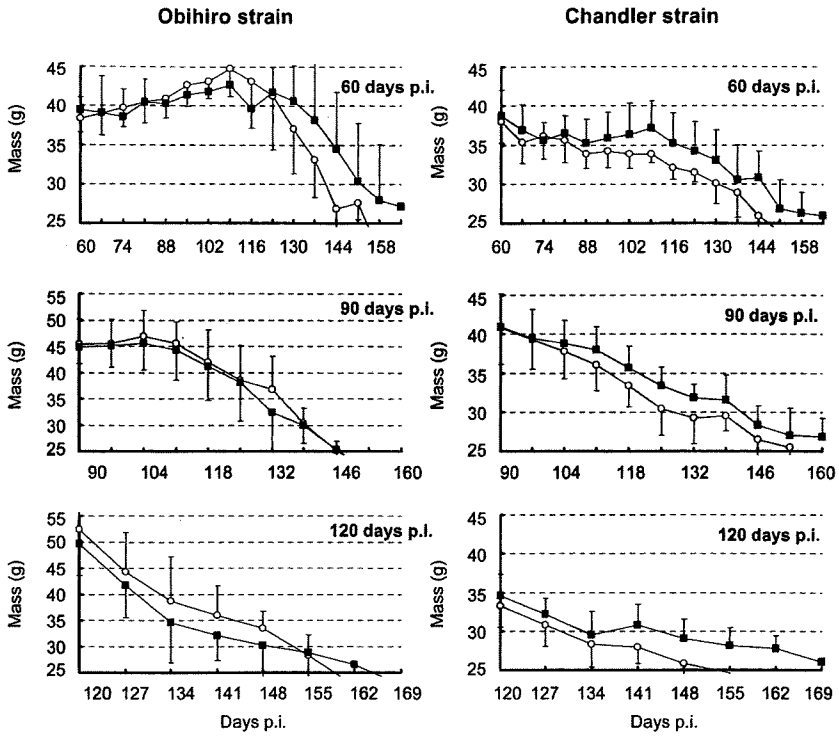

Fig. 6. Changes in body weight. After the initiation of mAb infusion, mice were weighed weekly up to the terminal stage of the disease. The groups of mice used in Fig. 5 were used to monitor body weight. ○, Mice treated with mAb P2-284; ■, mice treated with mAb 31C6.

to be milder than those observed in mice infused with the negative-control mAb. In contrast, no apparent reduction in microglial activation or astrogliosis by anti-PrP mAb was observed in the lateral cortex, where delivery of mAbs appeared to be inefficient (data not shown). It has been reported that the process of conversion of PrP^{C} to PrP^{Sc} on neurons rather than extracellular deposition of PrP^{Sc} is involved in neuronal degeneration (Brandner *et al.*, 1996; Mallucci *et al.*, 2003; Chesebro *et al.*, 2005). Although the mechanism by which PrP^{Sc} formation provokes microglial activation and astrogliosis remains to be elucidated, these results imply that arresting conversion of PrP^{C} to PrP^{Sc} via mAb infusion may contribute, at least to some extent, to the observed reduction in microglial activation and astrogliosis.

Previous results have shown that passive immunization with anti-PrP mAb via intraperitoneal injection does not have a protective effect after invasion of prion into the CNS or inoculation of prion via the intracerebral route (White *et al.*, 2003). In contrast, intraventricular infusion of anti-PrP mAb prolonged survival when mAb was infused at the time that PrP^{Sc} became detectable in the CNS (e.g. at 60 days p.i.). The difference seems to be explained by inadequate transfer of anti-PrP mAbs into the CNS across the blood–brain barrier when mAbs are administered peripherally. Several compounds, including amphotericin B, PPS, porphyrin derivatives and GN8, have been reported to prolong the survival of mice infected with prion when administered at the middle or late stage of infection, but the animals were still prior to clinical onset (Demaimay *et al.*, 1997; Doh-ura *et al.*, 2004; Kocisko *et al.*, 2006; Kuwata *et al.*, 2007). To the best of our knowledge, there has been only one report of a treatment that prolongs survival of animals already in the clinical phase. Specifically, intraperitoneal administration of MS-8209 was shown to prolong survival of mice infected with the C506M3 strain when treatment was carried out at the time of the appearance of neurological symptoms (Demaimay *et al.*, 1997). Human prion diseases are usually detected after clinical onset and thus the availability of treatments that are effective even after symptoms have begun to appear is highly important. Therefore, it is of interest that intraventricular infusion of anti-PrP mAb was effective for prolongation of survival, even when treatment was initiated after the appearance of early clinical signs (at 120 days p.i.) in mice infected with the Chandler strain. Although in this study mAb infusion for 14 days of duration achieved only 8 % prolongation, the result should encourage further trials with mAbs that may be useful in the development of therapeutic treatment for prion diseases. For instance, continuing treatment over a longer duration, which may keep the effective concentration of mAbs in the brain higher over a longer period of time, may improve the effect on survival. In addition, anti-PrP mAb prolonged survival, despite the fact that the infused mAb was not evenly distributed in the brain but rather was primarily restricted to the hippocampus and thalamus. Thus, it is conceivable that improved delivery of mAb might enhance the effects of anti-PrP mAb on survival. Fab and single-chain antibody fragments have also been shown to inhibit PrP^{Sc} formation (Peretz *et al.*, 2001; Donofrio *et al.*, 2005), and the smaller size of these fragments may be beneficial for efficient delivery in tissues.

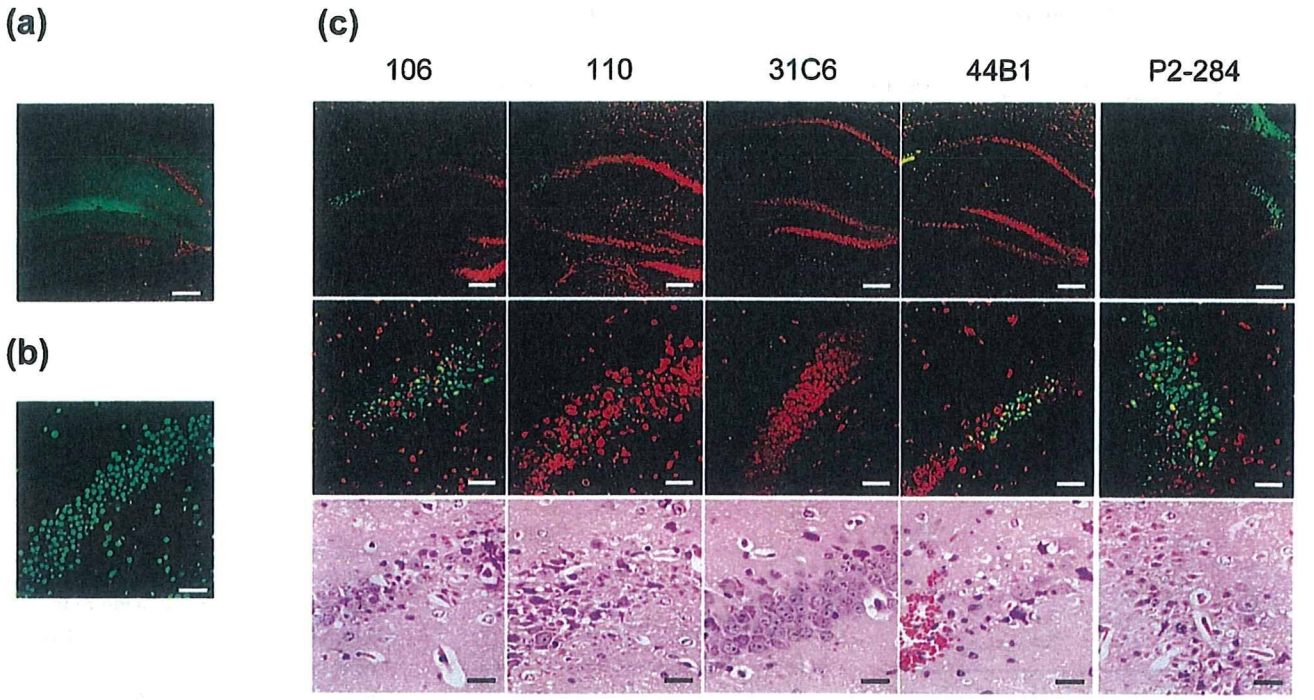

Fig. 7. Neuronal toxicity of anti-PrP mAbs. Anti-PrP mAbs (106, 110, 31C6 or 44B1) and the negative-control mAb P2-284 were injected into the left and right hippocampus, respectively, using stereotaxic apparatus. Seventy-two hours after injection, brains were obtained and fixed in 10% formalin. Paraffin sections were subjected to TUNEL and H&E staining. (a) Distribution of mAb. Alexa Fluor 488-conjugated mAb 31C6 was injected into the hippocampus and the distribution was analysed by confocal laser microscopy. (b) Positive control. Coronal sections were pre-treated with DNase I and then stained using the TUNEL procedure. The pyramidal cell layers of the hippocampus are shown. (c) TUNEL- and H&E-stained samples. Low-magnification (top panels) and high-magnification micrographs (middle panels) of TUNEL-stained samples and corresponding H&E-stained samples (bottom panels) are shown. The mAbs injected are indicated above the panels. Three to six mice were examined for each mAb. Bars, 200 μm.

Although mice infected with either the Obihiro or Chandler strain succumbed to the disease at around 150 days p.i., the effect of mAb infusion on survival differed when administered to mice challenged with different prion strains. For example, mAb infusion of mice infected with the Chandler strain was effective when the mAb was administered at any of the three time points tested (60, 90 and 120 days p.i.), whereas no prolongation was observed in mice infected with the Obihiro strain when mAb infusion was initiated at 90 or 120 days p.i. (Fig. 6). At present, we do not have a precise explanation for this but can speculate on what might explain the difference. First, microglial activation in mice infected with the Obihiro strain was more severe than that in mice infected with the Chandler strain (Figs 3 and 4). Similar to the mouse model for Alzheimer's disease (El Khoury *et al.*, 2007), microglial recruitment is expected to have a protective role in prion disease; however, activated microglia also have neurotoxic effects via production of cytokines, chemokines and reactive oxygen species (Bate *et al.*, 2001, 2002; Marella *et al.*, 2005). Thus, even when mitigated by anti-PrP mAb, the severe microglial activation in mice infected with Obihiro strain may be sufficient for progression of the disease. Secondly, differences in the distribution of PrP^{Sc} may account for the differences in the effect of anti-PrP mAb in one prion strain versus the other. For instance, PrP^{Sc} accumulation in the hypothalamus of mice infected with the Obihiro strain was more severe than that in mice infected with the Chandler strain (data not shown). Moreover, PrP^{Sc} formation in the hypothalamus might not be inhibited efficiently due to the uneven distribution of mAb in the hypothalamus (Fig. 1). These results may explain in part the lack of prolongation in the Obihiro strain-infected mice infused with mAb at 90 or 120 days p.i.

Immunotherapy has been of interest in the treatment of Alzheimer's disease; however, the fact that immunization of β-amyloid peptide caused meningoencephalitis in some patients in clinical trials warns of the adverse effects of autoimmune reactions *in vivo* (Check, 2002; Nicoll *et al.*, 2003; Orgogozo *et al.*, 2003). Additionally, cross-linking of PrP^{C} by an anti-PrP mAb that recognizes a specific epitope (aa 95–105) provoked degeneration of hippocampal and cerebellar neurons (Solforosi *et al.*, 2004). These adverse effects of antibodies on the CNS have prompted extreme

caution in the use of anti-PrP antibodies, in particular, their introduction into the CNS. However, passive immunization is less likely to initiate an autoimmune reaction (Schenk, 2002; Sadowski & Wisniewski, 2004). In this study, we observed no antibody-induced inflammation by intraventricular infusion. In addition, neuronal death in the hippocampus was not observed, even though mAbs 106 and 110, which recognize the region adjacent to aa 95–105, were injected directly into the hippocampus. Although the potential adverse effects, especially an inflammatory response, should be examined carefully, the fact that anti-PrP mAbs interfered with disease progression, even when administered after clinical onset, is particularly encouraging. Although the effect of anti-PrP mAb differed in prion strains, this implies that the immunotherapy might be effective in certain types of human prion disease, if not all. Therefore, the results of this study should promote further efforts to improve the effect of anti-PrP mAbs, such as the form of the antibody, the route of administration and an efficient way of delivering the antibodies.

ACKNOWLEDGEMENTS

This work was supported by the Regional New Consortium R&D Projects from the Ministry of Economy, Trade and Industry, a grant from The 21st Century COE Program (A-1) and a Grant-in-Aid for Science Research (A) (grant no. 18208026) from the Ministry of Education, Culture, Sports, Science and Technology of Japan. This work was also supported by a grant from the Ministry of Health, Labour and Welfare of Japan (grant no. 17270701). This work was also partly supported by a grant for Strategic Cooperation to Control Emerging and Re-emerging Infections and the Program of Founding Research Centers for Emerging and Reemerging Infectious Diseases, from the Ministry of Education, Culture, Sports, Science and Technology, Japan.

REFERENCES

Bate, C., Reid, S. & Williams, A. (2001). Killing of prion-damaged neurones by microglia. *Neuroreport* **12**, 2589–2594.

Bate, C., Boshuizen, R. S., Langeveld, J. P. & Williams, A. (2002). Temporal and spatial relationship between the death of PrP-damaged neurones and microglial activation. *Neuroreport* **13**, 1695–1700.

Brandner, S., Isenmann, S., Raeber, A., Fischer, M., Sailer, A., Kobayashi, Y., Marino, S., Weissmann, C. & Aguzzi, A. (1996). Normal host prion protein necessary for scrapie-induced neurotoxicity. *Nature* **379**, 339–343.

Check, E. (2002). Nerve inflammation halts trial for Alzheimer's drug. *Nature* **415**, 462.

Chesebro, B., Race, R. & Kercher, L. (2005). Scrapie pathogenesis in brain and retina: effects of prion protein expression in neurons and astrocytes. *J Neurovirol* **11**, 476–480.

Demaimay, R., Adjou, K. T., Beringue, V., Demart, S., Lasmézas, C. I., Deslys, J. P., Seman, M. & Dormont, D. (1997). Late treatment with polyene antibiotics can prolong the survival time of scrapie-infected animals. *J Virol* **71**, 9685–9689.

Doh-ura, K., Ishikawa, K., Murakami-Kubo, I., Sasaki, K., Mohri, S., Race, R. & Iwaki, T. (2004). Treatment of transmissible spongiform encephalopathy by intraventricular drug infusion in animal models. *J Virol* **78**, 4999–5006.

Donofrio, G., Heppner, F. L., Polymenidou, M., Musahl, C. & Aguzzi, A. (2005). Paracrine inhibition of prion propagation by anti-PrP single-chain Fv miniantibodies. *J Virol* **79**, 8330–8338.

Ehlers, B. & Diringer, H. (1984). Dextran sulphate 500 delays and prevents mouse scrapie by impairment of agent replication in spleen. *J Gen Virol* **65**, 1325–1330.

El Khoury, J., Toft, M., Hickman, S. E., Means, T. K., Terada, K., Geula, C. & Luster, A. D. (2007). Ccr2 deficiency impairs microglial accumulation and accelerates progression of Alzheimer-like disease. *Nat Med* **13**, 432–438.

Enari, M., Flechsig, E. & Weissmann, C. (2001). Scrapie prion protein accumulation by scrapie-infected neuroblastoma cells abrogated by exposure to a prion protein antibody. *Proc Natl Acad Sci U S A* **98**, 9295–9299.

Farquhar, C. F. & Dickinson, A. G. (1986). Prolongation of scrapie incubation period by an injection of dextran sulphate 500 within the month before or after infection. *J Gen Virol* **67**, 463–473.

Feraudet, C., Morel, N., Simon, S., Volland, H., Frobert, Y., Creminon, C., Vilette, D., Lehmann, S. & Grassi, J. (2005). Screening of 145 anti-PrP monoclonal antibodies for their capacity to inhibit PrP^{Sc} replication in infected cells. *J Biol Chem* **280**, 11247–11258.

Fernandez-Borges, N., Brun, A., Whitton, J. L., Parra, B., Diaz-San Segundo, F., Salguero, F. J., Torres, J. M. & Rodriguez, F. (2006). DNA vaccination can break immunological tolerance to PrP in wild-type mice and attenuates prion disease after intracerebral challenge. *J Virol* **80**, 9970–9976.

Furuoka, H., Yabuzoe, A., Horiuchi, M., Tagawa, Y., Yokoyama, T., Yamakawa, Y., Shinagawa, M. & Sata, T. (2005). Effective antigen-retrieval method for immunohistochemical detection of abnormal isoform of prion proteins in animals. *Acta Neuropathol* **109**, 263–271.

Gilch, S., Wopfner, F., Renner-Muller, I., Kremmer, E., Bauer, C., Wolf, E., Brem, G., Groschup, M. H. & Schatzl, H. M. (2003). Polyclonal anti-PrP auto-antibodies induced with dimeric PrP interfere efficiently with PrP^{Sc} propagation in prion-infected cells. *J Biol Chem* **278**, 18524–18531.

Goñi, F., Knudsen, E., Schreiber, F., Scholtzova, H., Pankiewicz, J., Carp, R., Meeker, H. C., Rubenstein, R., Brown, D. R. & other authors (2005). Mucosal vaccination delays or prevents prion infection via an oral route. *Neuroscience* **133**, 413–421.

Heppner, F. L., Musahl, C., Arrighi, I., Klein, M. A., Rülicke, T., Oesch, B., Zinkernagel, R. M., Kalinke, U. & Aguzzi, A. (2001). Prevention of scrapie pathogenesis by transgenic expression of anti-prion protein antibodies. *Science* **294**, 178–182.

Horiuchi, M. & Caughey, B. (1999). Specific binding of normal prion protein to the scrapie form via a localized domain initiates its conversion to the protease-resistant state. *EMBO J* **18**, 3193–3203.

Horiuchi, M., Yamazaki, N., Ikeda, T., Ishiguro, N. & Shinagawa, M. (1995). A cellular form of prion protein (PrP^{C}) exists in many non-neuronal tissues of sheep. *J Gen Virol* **76**, 2583–2587.

Horiuchi, M., Mochizuki, M., Ishiguro, N., Nagasawa, H. & Shinagawa, M. (1997). Epitope mapping of a monoclonal antibody specific to feline panleukopenia virus and mink enteritis virus. *J Vet Med Sci* **59**, 133–136.

Kaneko, K., Peretz, D., Pan, K. M., Blochberger, T. C., Wille, H., Gabizon, R., Griffith, O. H., Cohen, F. E., Baldwin, M. A. & Prusiner, S. B. (1995). Prion protein (PrP) synthetic peptides induce cellular PrP to acquire properties of the scrapie isoform. *Proc Natl Acad Sci U S A* **92**, 11160–11164.

Kim, C. L., Umetani, A., Matsui, T., Ishiguro, N., Shinagawa, M. & Horiuchi, M. (2004a). Antigenic characterization of an abnormal

isoform of prion protein using a new diverse panel of monoclonal antibodies. *Virology* **320**, 40–51.

Kim, C. L., Karino, A., Ishiguro, N., Shinagawa, M., Sato, M. & Horiuchi, M. (2004b). Cell-surface retention of PrP^C by anti-PrP antibody prevents protease-resistant PrP formation. *J Gen Virol* **85**, 3473–3482.

Kocisko, D. A., Caughey, W. S., Race, R. E., Roper, G., Caughey, B. & Morrey, J. D. (2006). A porphyrin increases survival time of mice after intracerebral prion infection. *Antimicrob Agents Chemother* **50**, 759–761.

Kuwata, K., Nishida, N., Matsumoto, T., Kamatari, Y. O., Hosokawa-Muto, J., Kodama, K., Nakamura, H. K., Kimura, K., Kawasaki, M. & other authors (2007). Hot spots in prion protein for pathogenic conversion. *Proc Natl Acad Sci U S A* **104**, 11921–11926.

Ladogana, A., Casaccia, P., Ingrosso, L., Cibati, M., Salvatore, M., Xi, Y. G., Masullo, C. & Pocchiari, M. (1992). Sulphate polyanions prolong the incubation period of scrapie-infected hamsters. *J Gen Virol* **73**, 661–665.

Mallucci, G., Dickinson, A., Linehan, J., Klöhn, P. C., Brandner, S. & Collinge, J. (2003). Depleting neuronal PrP in prion infection prevents disease and reverses spongiosis. *Science* **302**, 871–874.

Marella, M., Gaggioli, C., Batoz, M., Deckert, M., Tartare-Deckert, S. & Chabry, J. (2005). Pathological prion protein exposure switches on neuronal mitogen-activated protein kinase pathway resulting in microglia recruitment. *J Biol Chem* **280**, 1529–1534.

Morrissey, M. P. & Shakhnovich, E. I. (1999). Evidence for the role of PrP^C helix 1 in the hydrophilic seeding of prion aggregates. *Proc Natl Acad Sci U S A* **96**, 11293–11298.

Nicoll, J. A., Wilkinson, D., Holmes, C., Steart, P., Markham, H. & Weller, R. O. (2003). Neuropathology of human Alzheimer disease after immunization with amyloid-β peptide: a case report. *Nat Med* **9**, 448–452.

Orgogozo, J. M., Gilman, S., Dartigues, J. F., Laurent, B., Puel, M., Kirby, L. C., Jouanny, P., Dubois, B., Eisner, L. & other authors (2003). Subacute meningoencephalitis in a subset of patients with AD after Aβ42 immunization. *Neurology* **61**, 46–54.

Paxinos, G. & Franklin, K. B. J. (2001). *The Mouse Brain in Stereotaxic Coordinates*, 2nd edn. San Diego: Academic Press.

Peretz, D., Williamson, R. A., Kaneko, K., Vergara, J., Leclerc, E., Schmitt-Ulm, G., Mehlhorn, I. R., Legname, G., Wormald, M. R. & other authors (2001). Antibodies inhibit prion propagation and clear cell cultures of prion infectivity. *Nature* **412**, 739–743.

Perrier, V., Solassol, J., Crozet, C., Frobert, Y., Mourton-Gilles, C., Grassi, J. & Lehmann, S. (2004). Anti-PrP antibodies block PrP^{Sc} replication in prion-infected cell cultures by accelerating PrP^C degradation. *J Neurochem* **89**, 454–463.

Priola, S. A., Raines, A. & Caughey, W. S. (2000). Porphyrin and phthalocyanine antiscrapie compounds. *Science* **287**, 1503–1506.

Rainov, N. G., Tsuboi, Y., Krolak-Salmon, P., Vighetto, A. & Doh-Ura, K. (2007). Experimental treatments for human transmissible spongiform encephalopathies: is there a role for pentosan polysulfate? *Expert Opin Biol Ther* **7**, 713–726.

Sadowski, M. & Wisniewski, T. (2004). Vaccines for conformational disorders. *Expert Rev Vaccines* **3**, 279–290.

Schenk, D. (2002). Amyloid-β immunotherapy for Alzheimer's disease: the end of the beginning. *Nat Rev Neurosci* **3**, 824–828.

Schwarz, A., Krätke, O., Burwinkel, M., Riemer, C., Schultz, J., Henklein, P., Bamme, T. & Baier, M. (2003). Immunisation with a synthetic prion protein-derived peptide prolongs survival times of mice orally exposed to the scrapie agent. *Neurosci Lett* **350**, 187–189.

Sigurdsson, E. M., Brown, D. R., Daniels, M., Kascsak, R. J., Kascsak, R., Carp, R., Meeker, H. C., Frangione, B. & Wisniewski, T. (2002). Immunization delays the onset of prion disease in mice. *Am J Pathol* **161**, 13–17.

Solforosi, L., Criado, J. R., McGavern, D. B., Wirz, S., Sánchez-Alavez, M., Sugama, S., DeGiorgio, L. A., Volpe, B. T., Wiseman, E. & other authors (2004). Cross-linking cellular prion protein triggers neuronal apoptosis in vivo. *Science* **303**, 1514–1516.

Speare, J. O., Rush, T. S., III, Bloom, M. E. & Caughey, B. (2003). The role of helix 1 aspartates and salt bridges in the stability and conversion of prion protein. *J Biol Chem* **278**, 12522–12529.

Todd, N. V., Morrow, J., Doh-ura, K., Dealler, S., O'Hare, S., Farling, P., Duddy, M. & Rainov, N. G. (2005). Cerebroventricular infusion of pentosan polysulphate in human variant Creutzfeldt–Jakob disease. *J Infect* **50**, 394–396.

Trevitt, C. R. & Collinge, J. (2006). A systematic review of prion therapeutics in experimental models. *Brain* **129**, 2241–2265.

Uryu, M., Karino, A., Kamihara, Y. & Horiuchi, M. (2007). Characterization of prion susceptibility in Neuro2a mouse neuroblastoma cell subclones. *Microbiol Immunol* **51**, 661–667.

White, A. R., Enever, P., Tayebi, M., Mushens, R., Linehan, J., Brandner, S., Anstee, D., Collinge, J. & Hawke, S. (2003). Monoclonal antibodies inhibit prion replication and delay the development of prion disease. *Nature* **422**, 80–83.

Journal of General Virology (2010), 91, 563–569 DOI 10.1099/vir.0.016287-0

Short Communication

Cell density-dependent increase in the level of protease-resistant prion protein in prion-infected Neuro2a mouse neuroblastoma cells

Satoshi Nakamitsu, Aya Kurokawa, Takeshi Yamasaki, Masahide Uryu, Rie Hasebe and Motohiro Horiuchi

Correspondence
Motohiro Horiuchi
horiuchi@vetmed.hokudai.ac.jp

Laboratory of Prion Diseases, Graduate School of Veterinary Medicine, Hokkaido University, Kita 18, Nishi 9, Kita-ku, Sapporo 060-0818, Japan

Cells persistently infected with prions continuously produce protease-resistant prion protein (PrP-res). Here, we show that the PrP-res level in prion-infected Neuro2a (N2a) neuroblastoma cells decreased to 50 % of their initial level over the first 48 h and then recovered by 96 h after seeding. The level of cellular prion protein (PrP^C) also appeared to fluctuate, but did not influence the fluctuation of the PrP-res level. Prion-infected N2a cells, co-cultured with a higher number of prion-unsusceptible cells, had twice as much PrP-res as those cultured without unsusceptible cells, suggesting that cell density influences the fluctuation of PrP-res as. Direct cell-to-cell contact between cells, rather than soluble factors, was involved in the cell density-dependent increase in the PrP-res level. The cholesterol content, which is known to influence PrP-res formation, also changed depending on cell density. Our data suggest that alterations in cellular microenvironments controlled by cell density influence PrP-res formation.

Received 28 August 2009
Accepted 6 October 2009

The causative agent of prion diseases, prion, is believed to be composed mainly of an abnormal isoform of prion protein (PrP^{Sc}). During the progression of the disease, a host-encoded cellular prion protein (PrP^C) undergoes a conformational change to form PrP^{Sc}, which accumulates in the central nervous system. It is known that PrP^{Sc} is composed of protease-sensitive and -resistant forms (Tzaban *et al.*, 2002; Safar *et al.*, 2005; Pastrana *et al.*, 2006). The PrP^{Sc} form that is resistant to limited proteolysis is referred to as PrP-res, and PrP-res is used as a diagnostic marker of prion diseases.

Studies using prion-infected cells have provided many insights into prion biology, including the mechanism of PrP biosynthesis and the cell biological mechanism of prion propagation (Caughey & Raymond, 1991; Borchelt *et al.*, 1992; Vey *et al.*, 1996; Naslavsky *et al.*, 1997; Marijanovic *et al.*, 2009), and transmission of prions (Fevrier *et al.*, 2004; Gousset *et al.*, 2009; Mattei *et al.*, 2009). Although cells persistently infected with prions produce PrP-res and possess prion infectivity, the PrP-res level is known to change depending on the culture conditions, such as composition of the medium and differentiation state of cells (Rubenstein *et al.*, 1990; Bate *et al.*, 2004). The PrP-res level also changes during routine cell passage, possibly caused by subtle differences in the culture conditions.

PrP^{Sc} in prion-infected cells is believed to exist in a dynamic equilibrium between synthesis and degradation. Theoretically, after each cell division, the amount of PrP^{Sc} per cell must halve, after which it increases again to an appropriate level until the next cell division (Weissmann, 2004). Indeed, a decrease in PrP-res levels in cultured cells 48–72 h after passage followed by recovery of the PrP-res level thereafter has been reported (Ghaemmaghami *et al.*, 2007). During this process, certain host factors can modulate the equilibrium level of PrP^{Sc} by changing the rate of PrP-res formation, although the factors remain to be elucidated.

To understand the mechanism of fluctuation in the PrP-res levels in prion-infected cells, we analysed the kinetics of PrP-res levels in N2a subclones, N2a-5 and N2a-3 persistently infected with the Chandler strain (ScN2a-5-Ch and ScN2a-3-Ch; Uryu *et al.*, 2007). In addition, N2a-5 and N2a-3 cells persistently infected with the 22L strain (ScN2a-5-22L and ScN2a-3-22L) were used. Methods of immunoblotting and dot blotting for detecting PrP are described in Supplementary Material (available in JGV Online).

When ScN2a-5-Ch cells were seeded at a split ratio of 1 : 10, the culture was 40–50 % confluent 48 h after seeding, and 80–90 % confluent at 72 h after seeding (Fig. 1a). For analysing PrP-res levels, cells were first seeded into several 60 mm dishes at a 1 : 10 split ratio. At 72 h after seeding, the cells grown in one dish were harvested and used as the 0 h sample. Cells grown in other dishes were seeded again into new 60 mm dishes at a 1 : 10 or 1 : 40 split ratio, and

Supplementary material is available with the online version of this paper.

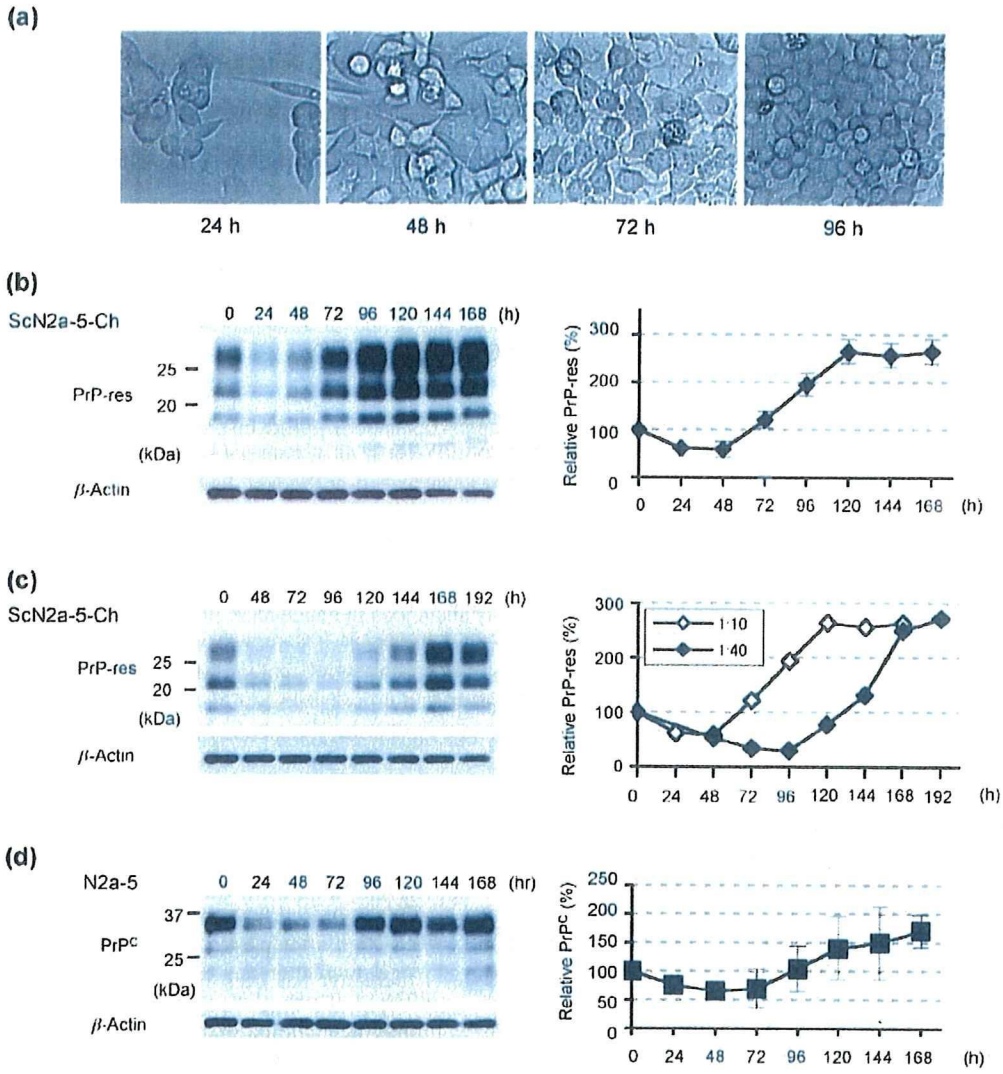

Fig. 1. Kinetics of the change in PrP levels in N2a subclone. (a) Phase-contrast microscopic images of ScN2a-5-Ch cells at the indicated culture times. (b) Changes in PrP-res levels in ScN2a-5-Ch cells. For the detection of β-actin, 10 μg post-nuclear cell lysates was loaded. For the detection of PrP-res, the cell lysates were treated with proteinase K (PK) and 100 μg cell lysate equivalents was loaded. The PrP-res level relative to that of PrP-res at 0 h was calculated, and graphs on the right represent the mean ± SD of the relative PrP-res levels (n=3). (c) The kinetics of PrP-res level in ScN2a-5-Ch cells passaged at a 1 : 40 split ratio (n=1, filled diamonds). Changes in the PrP-res level obtained after the passage at a 1 : 10 split ratio (open diamonds) were overlaid. (d) Changes in PrP^C levels in N2a-5 cells. Cell lysates (10 μg) without PK treatment were loaded. Graphs show the PrP^C level relative to the PrP^C level at 0 h (mean ± SD, n=3).

were harvested every 24 h for quantification of PrP-res by immunoblotting. In N2a-5 and N2a-3 cells infected with the Chandler strain, the level of PrP-res decreased to about 50 % of that of the 0 h PrP-res sample over the first 48 h, following which PrP-res levels recovered to the initial level by 72–96 h after seeding. If the cells were maintained in the same dishes thereafter, PrP-res levels further increased and then reached a plateau (Fig. 1b; Supplementary Fig. S1a, available in JGV Online). When ScN2a-5-Ch cells were seeded at a 1 : 40 split ratio, under which the cultures became confluent at 120–144 h after seeding, PrP-res levels began to increase from 96 h after seeding, and had recovered to the initial level by 120–144 h (Fig. 1c). This result indicates that fluctuation in the level of PrP-res does not simply depend on the time period after the seeding of cells. Although a pattern of the kinetic change of the PrP-res level in N2a cells infected with the 22L strain did not appear to be the same as that of the PrP-res level in the

Chandler-infected cells, the fluctuation in PrP-res level was also observed (Supplementary Fig. S1b, available in JGV Online).

The kinetics of PrP^C levels in N2a-5 and N2a-3 cells, especially by 96 h after seeding, were similar to those of PrP-res levels (Fig. 1d; Supplementary Fig. S1c, available in JGV Online). The PrP^C levels decreased to about 50% of that of the control (the amount of PrP^C at 0 h) over the first 48 h, but had recovered by 96 h after seeding, suggesting that fluctuation in the PrP-res level might be caused by a change in the level of PrP^C. However, the kinetics of PrP^C and PrP-res levels in PrP-overexpressing cells showed that even though the cells expressed a level of PrP^C that would be sufficient for PrP-res formation, the PrP-res level still decreased after seeding of the cells (Supplementary Fig. S2, available in JGV Online). Therefore, the observed fluctuation in the PrP-res level appears to be independent of that in the PrP^C level.

The results described above suggested that cell density is one of the factors for the increase in PrP-res level. To determine if cell density is indeed related to the increase in the PrP-res level, ScN2a-3-Ch cells were co-cultured with various numbers of N2a-1 cells to produce conditions under which the same number of ScN2a-3-Ch cells was present in cultures of different cell densities. N2a-1 cells express the same level of PrP^C as N2a-3 cells but are not susceptible to prions (Uryu *et al.*, 2007). Therefore, changes in the PrP-res level in these co-cultures should represent changes in PrP-res level in ScN2a-3-Ch cells.

First, we analysed the effect of the presence of N2a-1 cells at different densities on the growth of ScN2a-3-Ch cells. ScN2a-3-Ch cells, labelled with the PKH26 fluorescent dye, were co-cultured for 72 h with various numbers of N2a-1 cells (Fig. 2a). Counting of cells labelled with red revealed no significant difference in the number of ScN2a-3-Ch cells among co-cultures. This suggested that different numbers of counterpart cells did not influence the growth of ScN2a-3-Ch cells at least over 72 h. Therefore, the experimental condition was considered to be suitable for comparison of the PrP-res level in ScN2a-3-Ch cells cultured at different cell densities.

To analyse the effect of cell density on the PrP-res level, a uniform number of ScN2a-3-Ch cells (1 : 20 split ratio) was cultured for 3 days with various numbers of N2a-1 cells. ScN2a-3-Ch cells cultured with higher numbers of N2a-1 cells (Fig. 2b, 1 : 10 to 1 : 80 split ratio) had PrP-res at a level that was almost twice as high as the same number of ScN2a-3-Ch cells cultured in the absence of N2a-1 cells. These results suggest that a higher cell density facilitates PrP-res formation. Consistent with this observation, cells in areas with a higher cell density showed more intense fluorescence signals of PrP^{Sc} than cells with a lower cell density (Supplementary Fig. S3, available in JGV Online).

Since no difference was observed in the PrP-res levels in ScN2a-3-Ch cells cultured with or without the conditioned medium of N2a-1 cells grown at various densities (Fig. 2c), direct cell-to-cell contact rather than soluble factors is involved in the increase in PrP-res levels. In addition, co-culture of ScN2a-3-Ch cells with methanol-fixed N2a-1 cells did not increase PrP-res level (Fig. 2d), indicating that direct cell-to-cell contact between live cells is necessary for the increase in PrP-res levels. We further analysed the effect of PrP^C expression in the co-cultured counterpart cells on PrP-res formation, using N2a-24 cells that express trace levels of PrP^C (Uryu *et al.*, 2007). The cell density-dependent increase in PrP-res levels was again observed when ScN2a-3-Ch cells were cultured with high numbers of N2a-24 cells (Fig. 2e, 1 : 5 and 1 : 10 split ratio). We confirmed that the level of PrP^C in N2a-3 cells did not change under co-culture (Supplementary Fig. S4, available in JGV Online).

It has been reported that cellular cholesterol contents are increased in several cells when the cells reach confluency (Cansell *et al.*, 1997; Corvera *et al.*, 2000; Takahashi *et al.*, 2007). Since cholesterol depletion has been shown to affect PrP-res formation in prion-infected cell cultures (Taraboulos *et al.*, 1995; Bate *et al.*, 2004; Prior *et al.*, 2007), we first stained N2a-5 cells with filipin III, a sterol-binding polyene antibiotic. Stronger fluorescent intensities were observed in cells at a higher cell density than in cells at a lower cell density (Fig. 3a, compare cells at 24 and 96 h after seeding at 1 : 10 split ratio, or cells 72 h after seeding at 1 : 5 or 1 : 40 split ratio). Consistent with this observation, the cellular cholesterol content of subconfluent N2a-5 cells (Fig. 3b, 24 h after seeding) was about 25% less than that in confluent N2a-5 cells (96 h after seeding). In addition, the cholesterol content in N2a-5 cells seeded at a higher split ratio (Fig. 3c, 1 : 40) was lower than that in cells seeded at a lower split ratio (1 : 5). These results demonstrated that the cellular cholesterol content of N2a-5 cells increased when the cells reached confluency.

To examine whether an approximately 25% decrease in cellular cholesterol content influences PrP-res formation, cholesterol depletion was carried out with lovastatin or methyl-β-cyclodextrin (MβCD) under non-cytotoxic conditions (Fig. 3d). Lovastatin treatment resulted in 26% decrease in the cholesterol content of ScN2a-5-Ch cells. Under this condition, the level of PrP-res decreased to 45% of that of the untreated control. Thus, it is possible that the approximately 25% lower content of cholesterol in subconfluent N2a-5 cells affects PrP-res formation. In turn, the cholesterol content of nearly confluent, or confluent N2a cells, may be sufficient to maintain the level of PrP-res. On the contrary, MβCD treatment reduced cellular cholesterol content to 35% of that of untreated cells, which drastically reduced the level of PrP-res. Although MβCD is known to remove cholesterol from the cell membrane (Christian *et al.*, 1997; Simons *et al.*, 1998), MβCD also directly binds to PrP^C and inhibits the conversion of PrP^C to PrP-res (Prior *et al.*, 2007). Therefore, the efficient clearance of PrP-res appears to be due not only to cholesterol depletion, but also to a direct effect of MβCD on PrP^C.

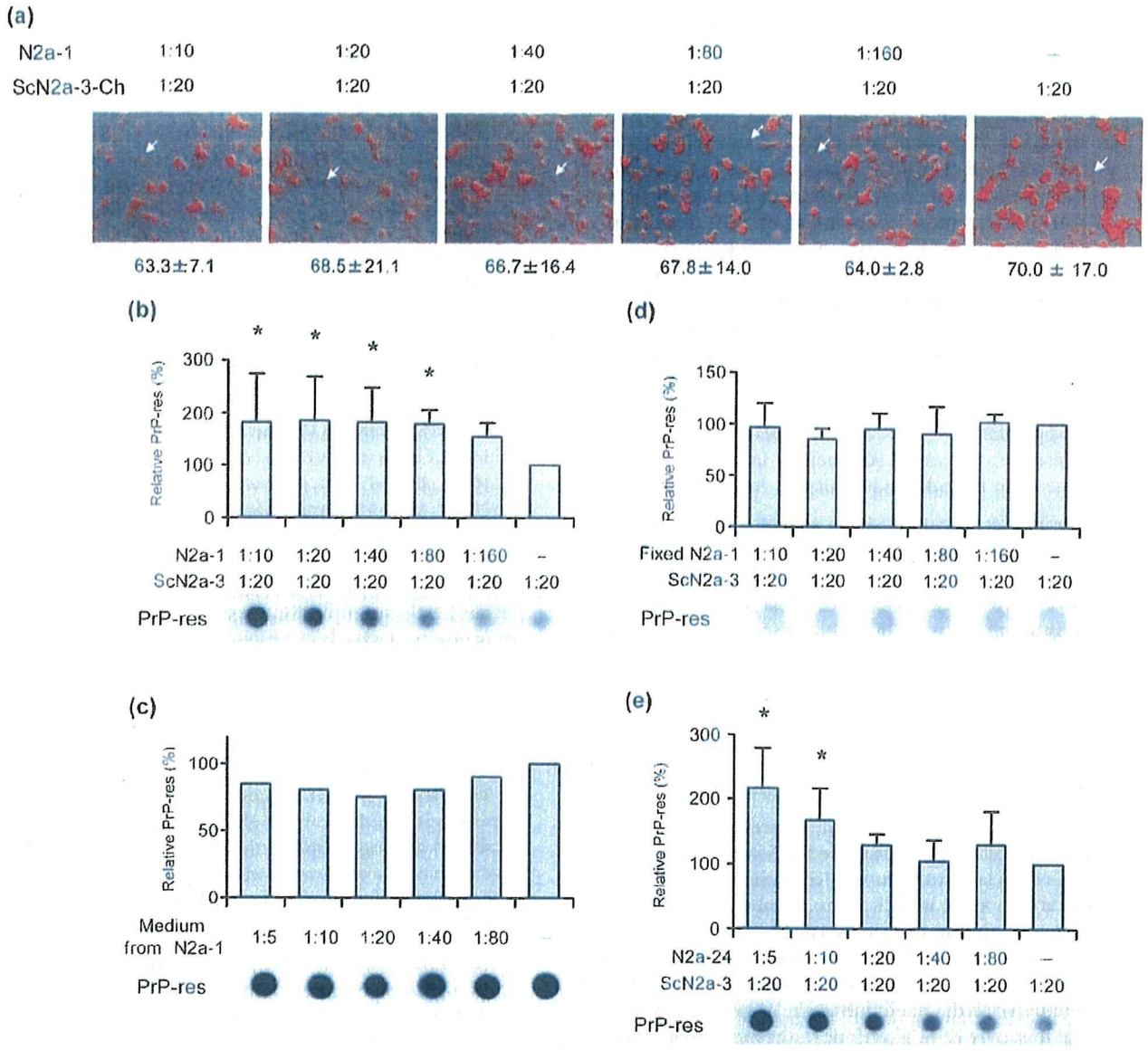

Fig. 2. Effect of cell density on PrP-res formation. (a) Co-cultured ScN2a-3-Ch cells with prion-unsusceptible N2a-1 cells. ScN2a-3-Ch cells labelled with PKH26 fluorescent dye (labelled with red) were co-cultured with various numbers of N2a-1 cells for 3 days. Phase-contrast images of the cells, overlaid with the corresponding fluorescent images, are shown. The ratios at the top indicate the split ratio of ScN2a-3-Ch and N2a-1 cells at seeding. The means ± SD of the number of labelled cells from four micrographs are shown below the images. The arrows indicate cells with threshold intensity that were counted as positive. For all (b–e), the PrP-res levels were measured by dot blotting and representative blots are shown. The split ratios of cells at seeding are indicated below each graph. (b) PrP-res levels in ScN2a-3-Ch cells co-cultured with N2a-1 cells for 3 days. The graph indicates the level of PrP-res relative to those in ScN2a-3-Ch cells without N2a-1 cells (n=4). Asterisks indicate significant difference (P<0.05) as analysed by Williams' multiple comparison test. (c) Effect of conditioned medium (CM). N2a-1 cells were seeded into 60 mm dishes at a 1 : 5 to 1 : 80 split ratio and cultured for 3 days. The supernatants (CM) were then harvested and filtered through a 0.22 μm filter. An equal volume of CM was added to ScN2a-3-Ch cells that were seeded at a 1 : 10 split ratio 24 h before the addition of CM, and the cells were incubated for an additional 48 h. The graph represents the level of PrP-res relative to the amount of PrP-res in ScN2a-3-Ch cells cultured without CM (n=1). (d) PrP-res levels in ScN2a-3-Ch cells co-cultured with fixed N2a-1 cells. N2a-1 cells seeded into 24-well-plates were cultured for 3 days and fixed with methanol. ScN2a-3-Ch cells were seeded at a 1 : 20 split ratio into wells containing fixed N2a-1 cells and cultured for 3 days. The graph shows the level of PrP-res relative to the amount of PrP-res in ScN2a-3-Ch cells without fixed N2a-1 (n=3). (e) PrP-res levels in ScN2a-3-Ch cells co-cultured with N2a-24 cells for 3 days (n=4). The co-culture was started at a ratio of 1 : 5 because growth rate of N2a-24 cells was slower than that of ScN2a-3 cells.

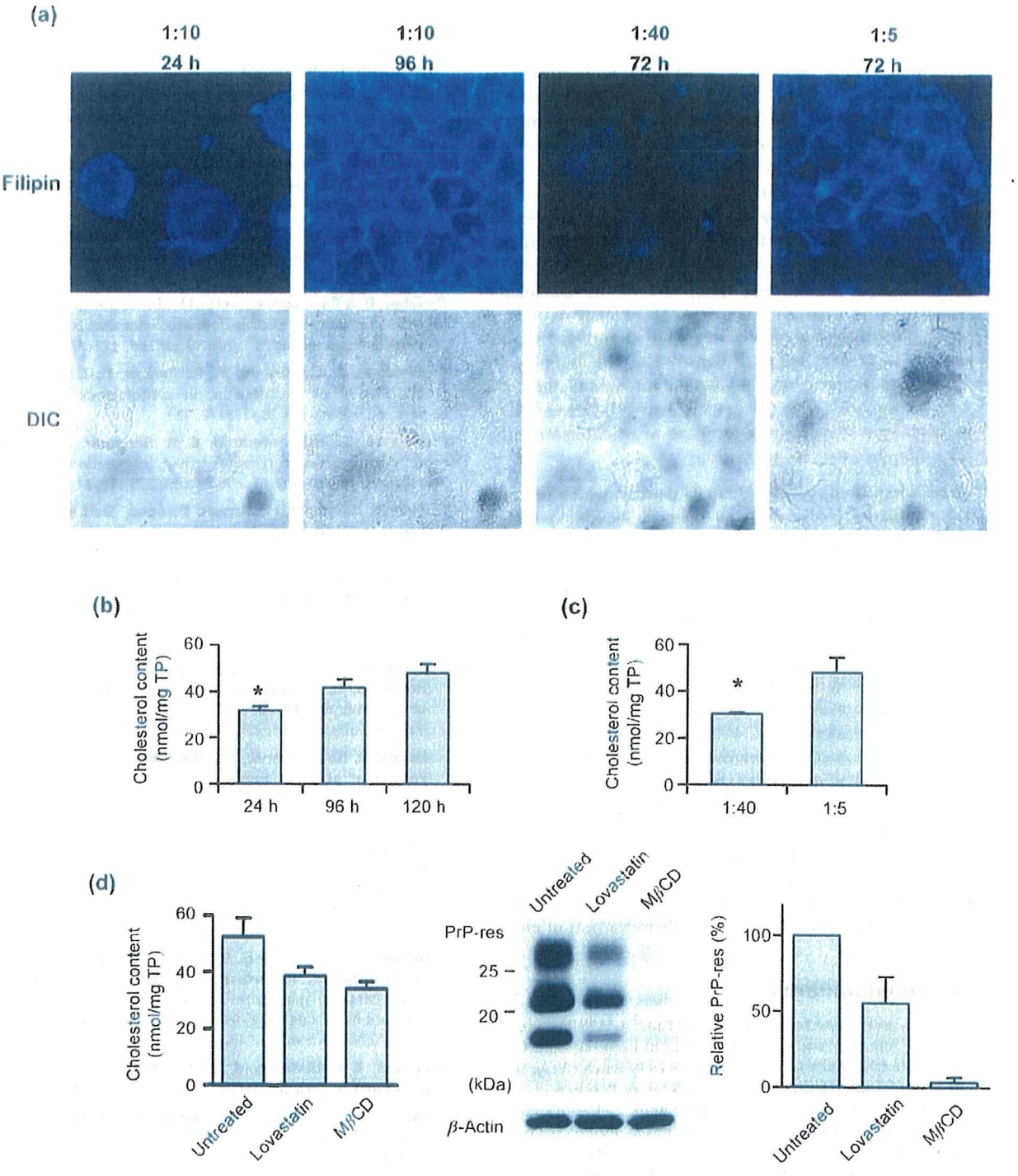

Fig. 3. The effect of cell density on cholesterol content. (a) Cellular localization of cholesterol. N2a-5 cells seeded at a 1 : 10 split ratio and cultured for 24 or 96 h, or cells seeded at a 1 : 5 or 1 : 40 split ratio and cultured for 72 h, were stained for cholesterol with filipin III. Top, fluorescence images; bottom, phase-contrast microscopic images. (b) Cholesterol content of subconfluent (24 h after seeding at a 1 : 10 split ratio) and confluent N2a-5 cells (96 and 120 h after seeding at a 1 : 10 split ratio). Cholesterol content is expressed as nmol per mg total protein (TP) ($n=3$). The asterisk indicates significant difference ($P<0.05$). (c) Cholesterol content of N2a-5 cells seeded at a 1 : 5 or 1 : 40 split ratio and cultured for 72 h. (d) Effect of cholesterol depletion on PrP-res formation. ScN2a-5-Ch cells were treated with 0.3 μM lovastatin or 2.0 μM MβCD for 96 h. The graph on the left indicates cholesterol content ($n=3$). The image in the middle is a representative immunoblot of PrP^{Sc} and corresponding β-actin, and the graph on the right shows the PrP-res level ($n=3$).

Cell confluency has also been reported to affect intracellular distribution of cholesterol in Chinese hamster ovary cells (Takahashi *et al.*, 2007). Treatment of prion-infected cells with a 24-dehydrocholesterol reductase inhibitor, U18666A, has been shown to inhibit PrP-res formation (Klingenstein *et al.*, 2006; Hagiwara *et al.*, 2007; Marijanovic *et al.*, 2009). Although treatment with U18666A did not appear to alter cellular cholesterol content (data not shown), U18666A inhibited intracellular cholesterol transport, resulting in a redistribution of cholesterol from the plasma membrane to intracellular compartments (Liscum & Underwood, 1995; Sparrow *et al.*, 1999; Klingenstein *et al.*, 2006). As shown in Fig. 3(a), N2a cells in an area of high cell density showed more intense cholesterol staining on the plasma membrane than N2a cells in an area with lower cell density. Therefore, cell density-dependent cellular localization of cholesterol may also influence PrP-res formation.

Here, we showed that a higher cell density, which increases the opportunity of cell-to-cell contact, facilitated PrP-res formation in prion-infected N2a cells. We also showed the possibility that cell density-dependent cholesterol content and/or localization may influence fluctuation in the PrP-res level. However, it remains to be clarified how cholesterol influences PrP-res formation that is controlled by cell density. Prion propagation in continuously dividing cultured cells differs from prion propagation in non-dividing neuronal cells in the central nervous system. However, the acceleration of PrP-res formation by direct cell-to-cell contact is somewhat analogous to the deposition of PrP^{Sc} at neuro-muscular junction (Andréoletti *et al.*, 2004; Thomzig *et al.*, 2004) or to synaptic deposition of PrP^{Sc} (Kitamoto *et al.*, 1992) in that specific and direct cell-to-cell interaction provides a niche for PrP-res formation. Further analysis of the cell density-dependent increase in PrP-res formation will provide clues for clarification of the environment that is required for PrP-res formation *in vivo*.

Acknowledgements

This work was supported by a Grant-in-Aid for JSPS Fellows (no. 20.7303). This work was supported by a grant from the Global COE Program (F-001) and a Grant-in-Aid for Science Research (A) (grant no. 18208026) and a Grant-in-Aid for Exploratory Research (grant no. 20658070) from the Ministry of Education, Culture, Sports, Science, and Technology of Japan. This work was also supported by a grant from the Ministry of Health, Labour and Welfare of Japan (grant no. 20330701, Research on Measures for Intractable Diseases). This work was also partly supported by a Grant-in-Aid from the BSE Control Project of the Ministry of Agriculture, Forestry and Fisheries of Japan, and the Program of Founding Research Centers for Emerging and Reemerging Infectious Diseases, from the Ministry of Education, Culture, Sports, Science, and Technology, Japan.

References

Andréoletti, O., Simon, S., Lacroux, C., Morel, N., Tabouret, G., Chabert, A., Lugan, S., Corbière, F., Ferré, P. & other authors (2004). PrP^{Sc} accumulation in myocytes from sheep incubating natural scrapie. *Nat Med* **10**, 591–593.

Bate, C., Langeveld, J. & Williams, A. (2004). Manipulation of PrPres production in scrapie-infected neuroblastoma cells. *J Neurosci Methods* **138**, 217–223.

Borchelt, D. R., Taraboulos, A. & Prusiner, S. B. (1992). Evidence for synthesis of scrapie prion proteins in the endocytic pathway. *J Biol Chem* **267**, 16188–16199.

Cansell, M., Gouygou, J. P., Jozefonvicz, J. & Letourneur, D. (1997). Lipid composition of cultured endothelial cells in relation to their growth. *Lipids* **32**, 39–44.

Caughey, B. & Raymond, G. J. (1991). The scrapie-associated form of PrP is made from a cell surface precursor that is both protease- and phospholipase-sensitive. *J Biol Chem* **266**, 18217–18223.

Christian, A. E., Haynes, M. P., Phillips, M. C. & Rothblat, G. H. (1997). Use of cyclodextrins for manipulating cellular cholesterol content. *J Lipid Res* **38**, 2264–2272.

Corvera, S., DiBonaventura, C. & Shpetner, H. S. (2000). Cell confluence-dependent remodeling of endothelial membranes mediated by cholesterol. *J Biol Chem* **275**, 31414–31421.

Fevrier, B., Vilette, D., Archer, F., Loew, D., Faigle, W., Vidal, M., Laude, H. & Raposo, G. (2004). Cells release prions in association with exosomes. *Proc Natl Acad Sci U S A* **101**, 9683–9688.

Ghaemmaghami, S., Phuan, P., Perkins, B., Ullman, J., May, B. C. H., Cohen, F. E. & Prusiner, S. B. (2007). Cell division modulates prion accumulation in cultured cells. *Proc Natl Acad Sci U S A* **104**, 17971–17976.

Gousset, K., Schiff, E., Langevin, C., Marijanovic, Z., Caputo, A., Browman, D. T., Chenouard, N., de Chaumont, F., Martino, A. & other authors (2009). Prions hijack tunnelling nanotubes for intercellular spread. *Nat Cell Biol* **11**, 328–336.

Hagiwara, K., Nakamura, Y., Nishijima, M. & Yamakawa, Y. (2007). Prevention of prion propagation by dehydrocholesterol reductase inhibitors in cultured cells and a therapeutic trial in mice. *Biol Pharm Bull* **30**, 835–838.

Kitamoto, T., Shin, R. W., Doh-ura, K., Tomokane, N., Miyazono, M., Muramoto, T. & Tateishi, J. (1992). Abnormal isoform of prion proteins accumulates in the synaptic structures of the central nervous system in patients with Creutzfeldt–Jakob disease. *Am J Pathol* **140**, 1285–1294.

Klingenstein, R., Löber, S., Kujala, P., Godsave, S., Leliveld, S. R., Gmeiner, P., Peters, P. J. & Korth, C. (2006). Tricyclic antidepressants, quinacrine and a novel, synthetic chimera thereof clear prions by destabilizing detergent-resistant membrane compartments. *J Neurochem* **98**, 748–759.

Liscum, L. & Underwood, K. W. (1995). Intracellular cholesterol transport and compartmentation. *J Biol Chem* **270**, 15443–15446.

Marijanovic, Z., Caputo, A., Campana, V. & Zurzolo, C. (2009). Identification of an intracellular site of prion conversion. *PLoS Pathog* **5**, e1000426.

Mattei, V., Barenco, M. G., Tasciotti, V., Garofalo, T., Longo, A., Boller, K., Löwer, J., Misasi, R., Montrasio, F. & Sorice, M. (2009). Paracrine diffusion of PrP(C) and propagation of prion infectivity by plasma membrane-derived microvesicles. *PLoS One* **4**, e5057.

Naslavsky, N., Stein, R., Yanai, A., Friedlander, G. & Taraboulos, A. (1997). Characterization of detergent-insoluble complexes containing the cellular prion protein and its scrapie isoform. *J Biol Chem* **272**, 6324–6331.

Pastrana, M. A., Sajnani, G., Onisko, B., Castilla, J., Morales, R., Soto, C. & Requena, J. R. (2006). Isolation and characterization of a proteinase K-sensitive PrP^{Sc} fraction. *Biochemistry* **45**, 15710–15717.

Prior, M., Lehmann, S., Sy, M., Molloy, B. & McMahon, H. E. M. (2007). Cyclodextrins inhibit replication of scrapie prion protein in cell culture. *J Virol* **81**, 11195–11207.

Rubenstein, R., Scalici, C. L., Papini, M. C., Callahan, S. M. & Carp, R. I. (1990). Further characterization of scrapie replication in PC12 cells. *J Gen Virol* **71**, 825–831.

Safar, J. G., Geschwind, M. D., Deering, C., Didorenko, S., Sattavat, M., Sanchez, H., Serban, A., Vey, M., Baron, H. & other authors (2005). Diagnosis of human prion disease. *Proc Natl Acad Sci U S A* **102**, 3501–3506.

Simons, M., Keller, P., De Strooper, B., Beyreuther, K., Dotti, C. G. & Simons, K. (1998). Cholesterol depletion inhibits the generation of beta-amyloid in hippocampal neurons. *Proc Natl Acad Sci U S A* **95**, 6460–6464.

Sparrow, S. M., Carter, J. M., Ridgway, N. D., Cook, H. W. & Byers, D. M. (1999). U18666A inhibits intracellular cholesterol transport and neurotransmitter release in human neuroblastoma cells. *Neurochem Res* **24**, 69–77.

Takahashi, M., Murate, M., Fukuda, M., Sato, S. B., Ohta, A. & Kobayashi, T. (2007). Cholesterol controls lipid endocytosis through Rab11. *Mol Biol Cell* **18**, 2667–2677.

Taraboulos, A., Scott, M., Semenov, A., Avrahami, D., Laszlo, L., Prusiner, S. B. & Avraham, D. (1995). Cholesterol depletion and modification of COOH-terminal targeting sequence of the prion protein inhibit formation of the scrapie isoform. *J Cell Biol* **129**, 121–132.

Thomzig, A., Schulz-Schaeffer, W., Kratzel, C., Mai, J. & Beekes, M. (2004). Preclinical deposition of pathological prion protein PrP^{Sc} in muscles of hamsters orally exposed to scrapie. *J Clin Invest* **113**, 1465–1472.

Tzaban, S., Friedlander, G., Schonberger, O., Horonchik, L., Yedidia, Y., Shaked, G., Gabizon, R. & Taraboulos, A. (2002). Protease-sensitive scrapie prion protein in aggregates of heterogeneous sizes. *Biochemistry* **41**, 12868–12875.

Uryu, M., Karino, A., Kamihara, Y. & Horiuchi, M. (2007). Characterization of prion susceptibility in Neuro2a mouse neuroblastoma cell subclones. *Microbiol Immunol* **51**, 661–669.

Vey, M., Pilkuhn, S., Wille, H., Nixon, R., DeArmond, S. J., Smart, E. J., Anderson, R. G., Taraboulos, A. & Prusiner, S. B. (1996). Subcellular colocalization of the cellular and scrapie prion proteins in caveolae-like membranous domains. *Proc Natl Acad Sci U S A* **93**, 14945–14949.

Weissmann, C. (2004). The state of the prion. *Nat Rev Microbiol* **2**, 861–871.

JOURNAL OF VIROLOGY, June 2009, p. 5918–5927 Vol. 83, No. 11
0022-538X/09/$08.00+0 doi:10.1128/JVI.00165-09

Effect of Transplantation of Bone Marrow-Derived Mesenchymal Stem Cells on Mice Infected with Prions▽†

Chang-Hyun Song,[1] Osamu Honmou,[2] Natsuo Ohsawa,[1] Kiminori Nakamura,[3] Hirofumi Hamada,[3] Hidefumi Furuoka,[4] Rie Hasebe,[1] and Motohiro Horiuchi[1]*

Laboratory of Prion Diseases, Graduate School of Veterinary Medicine, Hokkaido University, Kita 18, Nishi 9, Kita-ku, Sapporo 060-0818,[1] Departments of Neural Repair and Therapeutics[2] and Molecular Medicine,[3] Sapporo Medical University, South-1st, West-16th, Chuo-ku, Sapporo 060-8543, and Department of Pathobiological Science, Obihiro University of Agriculture and Veterinary Medicine, Inada-cho, Obihiro 080-8555, Japan[4]

Received 23 January 2009/Accepted 9 March 2009

Bone marrow-derived mesenchymal stem cells (MSCs) have been reported to migrate to brain lesions in experimental models of ischemia, tumors, and neurodegenerative diseases and to ameliorate functional deficits. In this study, we attempted to evaluate the therapeutic potential of MSCs for treating prion diseases. Immortalized human MSCs (hMSCs) that express the *LacZ* gene were transplanted into the unilateral hippocampi or thalami of mice, and their distributions were monitored by the expression of β-galactosidase. In mice infected with prions, hMSCs transplanted at 120 days postinoculation (dpi) were detected on the contralateral side at 2 days after transplantation and existed there even at 3 weeks after transplantation. In contrast, few hMSCs were detected on the contralateral side for mock-infected mice. Interestingly, the migration of hMSCs appeared to correlate with the severity of neuropathological lesions, including disease-specific prion protein deposition. The hMSCs also migrated to a prion-specific lesion in the brain, even when intravenously injected. Although the effects were modest, intrahippocampal and intravenous transplantation of hMSCs prolonged the survival of mice infected with prions. A subpopulation of hMSCs in the brains of prion-infected mice produced various trophic factors and differentiated into cells of neuronal and glial lineages. These results suggest that MSCs have promise as a cellular vehicle for the delivery of therapeutic genes to brain lesions associated with prion diseases and, furthermore, that they may help to regenerate neuronal tissues damaged by prion propagation.

Prion diseases are fatal neurodegenerative disorders of humans and animals that are strongly associated with the conversion of normal prion protein (PrP^{C}) to a disease-specific isoform of prion protein (PrP^{Sc}). Many inhibitors of PrP^{Sc} formation, investigated by using cells persistently infected with prions or an in vitro conversion reaction, have been reported as candidates for therapeutics (55). Several compounds or active/passive immunization with PrP showed a prophylactic effect when administered before, simultaneously with, or just after inoculation with prions (14, 19, 43, 50, 52). However, only a few compounds, such as amphotericin B and its derivative pentosan polysulfate, porphyrin derivatives, and certain amyloidophilic compounds, have been shown to be effective at prolonging survival when administered in the middle or late stage of prion infection (10, 13, 25, 27). In clinical trials, pentosan polysulfate seems to extend the survival of several patients beyond the mean but appears unable to arrest the progression of the disease (4, 45).

Recently, we demonstrated that intraventricular infusion of an anti-PrP monoclonal antibody (MAb) could antagonize disease progression even when initiated after clinical onset, although the distribution of the MAb was largely restricted to the hippocampus and thalamus (53). Thus, improved delivery of the MAb may enhance its beneficial effects. Additionally, because antagonizing PrP^{Sc} formation is not sufficient to restore degenerated lesions, it is necessary to pursue ways to regenerate degenerated neuronal tissues.

Bone marrow-derived mesenchymal stem cells (MSCs) are multipotent adult stem cells of mesodermal origin. They can differentiate into mesenchymal lineages, such as osteoblasts, adipocytes, and myocytes (15, 41, 44). Remarkably, they also *trans*-differentiate into nonmesodermal cell types, including neuronal and glial lineages (48, 61). A number of studies have shown that MSCs migrate to damaged neuronal tissues following cerebral or systemic transplantation in animal models of ischemia (2, 7), spinal cord injury (23), brain tumors (37), Parkinson's diseases (21, 30), and Niemann-Pick disease (24). The introduction of MSCs in these model contexts resulted in functional recovery; however, the precise mechanisms for restoration remain to be elucidated (36, 38).

In this study, we investigated the therapeutic potential of MSCs for prion diseases. Although the use of mouse MSCs is suitable for studying the effect of MSCs on mice infected with prions, we used immortalized human MSCs (hMSCs) here because of the lack of appropriate methods for the isolation of mouse MSCs at the beginning of the study. In addition, hMSCs can be readily expanded in cell culture; their phenotypes remain similar to those of the primary human MSCs (26); and

* Corresponding author. Mailing address: Laboratory of Prion Diseases, Graduate School of Veterinary Medicine, Hokkaido University, Kita 18, Nishi 9, Kita-ku, Sapporo 060-0818, Japan. Phone and fax: 81-11-706-5293. E-mail: horiuchi@vetmed.hokudai.ac.jp.

† Supplemental material for this article may be found at http://jvi.asm.org/.

▽ Published ahead of print on 18 March 2009.

hMSCs are reported to avoid allogeneic rejection when they are transplanted into rat brains in a model of ischemia (38). Here we show that the hMSCs can migrate to neuropathological lesions in prion-infected mice and that their transplantation prolongs the survival of such mice. In addition, we also show that hMSCs that have migrated to prion-specific lesions secrete trophic factors and differentiate into cells of neuronal and glial lineages.

MATERIALS AND METHODS

MSCs. A retroviral vector, Rx-LacZ-bsr, containing the expression units of the *lacZ* gene and a gene conferring blasticidin resistance, were generated as described elsewhere (63). The recombinant retrovirus was used to transfect human bone marrow-derived MSCs that had been immortalized with the human telomerase catalytic subunit gene (26), and hMSCs were selected in the presence of 10 μg/ml of blasticidin. hMSCs stably expressing β-galactosidase (β-Gal) were cultured with Dulbecco's modified Eagle medium (DMEM) (Sigma Chemical Co., St. Louis, MO) containing 10% fetal bovine serum under a humidified atmosphere of 5% CO_2 at 37°C.

Mice and prion inoculation. Animal experiments were performed according to protocols approved by the Institutional Committee for Animal Experiments. Four-week-old female Jcl:ICR mice were purchased from CLEA Japan, and all mice were acclimatized for a week prior to use. Mice were intracerebrally inoculated with 20 μl of a 10% (wt/vol) brain homogenate from Jcl:ICR mice infected with the scrapie strain Obihiro or Chandler. Mice assigned to the mock-infected group were intracerebrally inoculated with 20 μl of a 10% (wt/vol) brain homogenate from age-matched uninfected Jcl:ICR mice. All mice were maintained on ad libitum feed and water with a 12-h light/dark cycle.

Transplantation of hMSCs. For transplantation of cells into the hippocampus or thalamus, mice were anesthetized by intramuscular injection of xylazine (10 mg/kg) and ketamine (50 mg/kg) and were placed on a stereotaxic apparatus (Narishige, Japan). After a linear scalp incision, burr holes were drilled to accommodate stereotaxic placement into the left hippocampus (2.0 mm caudal and 2.1 mm lateral to the bregma; depth, 2 mm) or thalamus (2.0 mm caudal and 1.5 mm lateral to the bregma; depth, 3.2 mm). hMSCs (1×10^5 cells in 2 μl phosphate-buffered saline [PBS]) were transplanted over a period of 15 min using a Hamilton syringe with a 31-gauge needle set in a micromanipulator. For transplantation of hMSCs via a peripheral route, 1×10^6 hMSCs were injected intravenously through the tail vein.

Immunohistochemistry. Mouse brains were frozen in Tissue-Tek OCT compound (Sakura, Japan), and cryosections (10 μm thick) were prepared as described elsewhere (53). Coronal sections were dried and fixed with ice-cold methanol for 15 min. A mouse anti-β-Gal MAb (catalog no. Z3783; Promega, Madison, WI) was conjugated with Alexa Fluor 488 by using a protein labeling kit (Molecular Probes, Eugene, OR) for the detection of hMSCs by direct staining. The following antibodies were used for the detection of various tropic factors: rabbit polyclonal antibodies against nerve growth factor (NGF) (Santa Cruz Biotechnology, Santa Cruz, CA), brain-derived neurotropic factor (BDNF) (Chemicon, Temecula, CA), neurotrophin 3 (NT3) (Chemicon), and neurotrophin 4/5 (NT4/5) (Santa Cruz Biotechnology); a rabbit MAb against vascular endothelial growth factor (VEGF) (clone EP1176Y; Abcam, Cambridge, MA); and a mouse MAb against ciliary neurotropic factor (CNTF) (clone A-11; Santa Cruz Biotechnology). As neuronal markers, we used a mouse MAb against microtubule-associated protein 2 (MAP2) (clone HM-2; Sigma Chemical Co.) for neurons, rabbit polyclonal antibodies (Dako, Denmark) against glial fibrillary acidic protein (GFAP) for astrocytes, and a mouse MAb against cyclic nucleotide phosphodiesterase (CNPase) (clone 11-5B; Chemicon) for oligodendrocytes. All sections were incubated with primary antibodies for 1 h at 37°C. To detect trophic factors and neural markers, the sections were subsequently incubated with an Alexa Fluor 546-conjugated anti-mouse antibody or an Alexa Fluor 555-conjugated anti-rabbit antibody (Molecular Probes) for 1 h at room temperature. After a wash with PBS, sections were mounted with Vectashield containing propidium iodide or 4′,6-diamidino-2-phenylindole (DAPI; Vector Laboratories, Burlingame, CA) and were examined with a Nikon C1 laser confocal microscope. To exclude the possibility of nonspecific reactions between the Alexa Fluor 546-conjugated anti-mouse antibody and mouse tissues, we carried out the immunostaining without primary antibodies and confirmed that the level of nonspecific binding of the Alexa Fluor 546-conjugated anti-mouse antibody was negligible.

For the detection of PrP^{Sc} accumulation and astrocytosis, mouse brains were fixed in 10% formalin and embedded in paraffin. Coronal sections (thickness, 4 μm) were subjected to hematoxylin-eosin (HE) staining or immunohistochemistry as described elsewhere (17, 53).

Proliferation assay. To detect proliferating cells in the brain, 50 mg of bromodeoxyuridine (BrdUrd; Sigma Chemical Co.) per kg of body weight in PBS with 0.007 M NaOH was administered to mice intraperitoneally twice a day for a week. BrdUrd administration was initiated soon or 2 weeks after the transplantation of hMSCs into the hippocampus. Mice were sacrificed 24 h after the last BrdUrd administration, and the brains of these mice were then prepared for cryosectioning. The sections were pretreated with 2 M HCl for 30 min at 37°C, followed by a neutralization step with 0.1 M borate buffer for 15 min at room temperature. BrdUrd in nuclei was detected using a fluorescein isothiocyanate-conjugated anti-BrdUrd MAb (clone B33.1; Abcam).

Cell migration assay. Prion- or mock-infected mice were sacrificed at 120 days postinoculation (dpi), and the brains of these mice were homogenized to 20% in DMEM (Sigma Chemical Co.). The homogenates were centrifuged at 10,000 × *g* for 10 min at 4°C, and the resulting supernatants were filtered (pore size, 0.22 μm). The brain extracts were aliquoted and stored at −80°C until use. Migration of hMSCs to brain extracts was analyzed using a QCM 24-well colorimetric cell migration assay kit (Chemicon). The hMSCs (approximately 80% confluent) were starved by incubation with serum-free medium 1 day before use. Then hMSCs were harvested, and a cell suspension (5×10^4 cells) was added to the insert well. The lower chambers were supplied with serum-free DMEM containing 1.0 or 0.1% brain extract. Twenty-four hours after incubation, hMSCs that had migrated through the polycarbonate membrane were extracted, and the absorbance at 560 nm was measured according to the manufacturer's instructions.

RESULTS

Distribution of hMSCs to the neuropathological lesions of prion disease. To test if hMSCs migrate to brain lesions caused by prion infection, we transplanted hMSCs into the left hippocampi of prion- or mock-infected mice at 120 dpi and monitored the distribution of β-Gal-positive hMSCs at 2 days and 1, 2, and 3 weeks after transplantation. In mock-infected mice, hMSCs were detected in the left hippocampus (transplanted side), but few hMSCs were detected in the contralateral hippocampus at 2 days to 3 weeks after transplantation (Fig. 1a). In contrast, hMSCs were detected both on the transplanted sides and on the contralateral sides of the hippocampi of mice infected with strain Chandler even 2 days after transplantation. Thereafter, hMSCs were constantly observed on both sides of the hippocampus during the observation period (every week after transplantation up to 3 weeks [Fig. 1a]). For each experimental group, we examined three mice at each time point and confirmed the similar results. One to 3 weeks after transplantation, hMSCs were also detected in the cortices, cerebella, medullae oblongatae (see Fig. 3b), and thalami (data not shown) of mice infected with prions, where intense PrP^{Sc} accumulations and astrocytosis were observed (see Fig. S1 in the supplemental material). Ramified hMSCs were observed in the corpus callosum; their morphologies differed from those observed in the contralateral hippocampus (Fig. 1b).

Transplantation of hMSCs into the left thalamus led to similar results. In mock-infected mice, hMSCs remained in the transplanted area, and few hMSCs migrated to the contralateral thalamus or to other regions. In contrast, many hMSCs were detected in the contralateral thalami (Fig. 1c) and hippocampi (data not shown) of mice infected with prions by 3 weeks posttransplantation.

We noticed a striking difference in the neuropathology of the hypothalami of mice infected with strain Obihiro versus strain Chandler. Specifically, PrP^{Sc} accumulations, astrocytosis, and spongiosis in the hypothalami of mice infected with

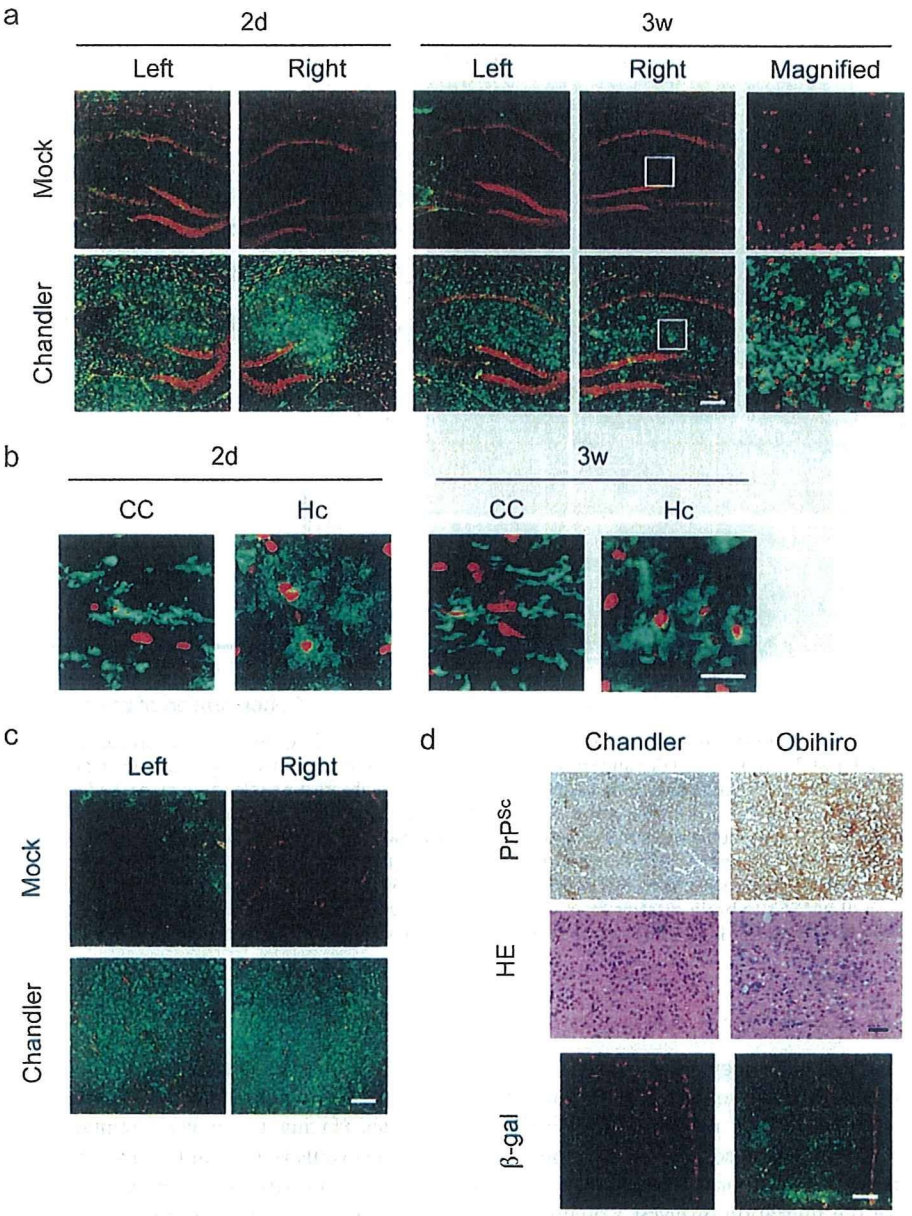

FIG. 1. Distribution of hMSCs to the neuropathological lesions of prion disease. At 120 dpi, hMSCs (1×10^5 cells) were transplanted into the left hippocampi or thalami of mice infected with strain Chandler and into those of age-matched mock-infected mice. Mice were sacrificed at 2 days or at 1, 2, or 3 weeks posttransplantation. Cryosections were stained with an Alexa Fluor 488-conjugated anti-β-Gal MAb (green) and counterstained with propidium iodide (red). (a) hMSCs in the hippocampus. Ipsilateral (left) and contralateral (right) hippocampi 2 days (2d) and 3 weeks (3w) posttransplantation are shown. The rightmost panels show magnified images of the regions boxed in the panels immediately to the left. Bar, 200 μm. (b) Morphology of hMSCs in the corpora callosa (CC) and contralateral hippocampi (Hc) of mice infected with strain Chandler at 2 days and 3 weeks posttransplantation. Bar, 20 μm. (c) hMSCs in the thalamus. Ipsilateral (left) and contralateral (right) thalami 3 weeks posttransplantation are shown. Bar, 200 μm. (d) Migration of hMSCs to the hypothalamus. (Top and center) Results of immunostaining for PrP^{Sc} and HE staining of the hypothalami of mice infected with strain Obihiro or Chandler are shown at 150 dpi. Bar, 100 μm. (Bottom) The hMSCs were detected in the hypothalamus (β-Gal) 3 weeks after transplantation into the left hippocampus. Bar, 200 μm.

strain Obihiro are more severe than those for mice infected with strain Chandler (Fig. 1d; see also Fig. S1 in the supplemental material). Consistent with the severity of neuropathological lesions, more hMSCs migrated to the hypothalami of mice infected with strain Obihiro than to those of mice infected with strain Chandler (Fig. 1d; β-Gal). These results suggest that hMSCs are capable of migrating to brain lesions caused by prion infection.

Migration of hMSCs in response to prion-specific lesions. To confirm the migration of hMSCs to lesions where PrP^{Sc} accumulates, we transplanted hMSCs into the left hippocampi of mice infected with strain Chandler at 73, 100, and 120 dpi, and we analyzed their migration to the contralateral (right) side a week after transplantation. When hMSCs were transplanted at 73 dpi, many hMSCs were detected on the transplanted side but fewer hMSCs were detected in the contralat-

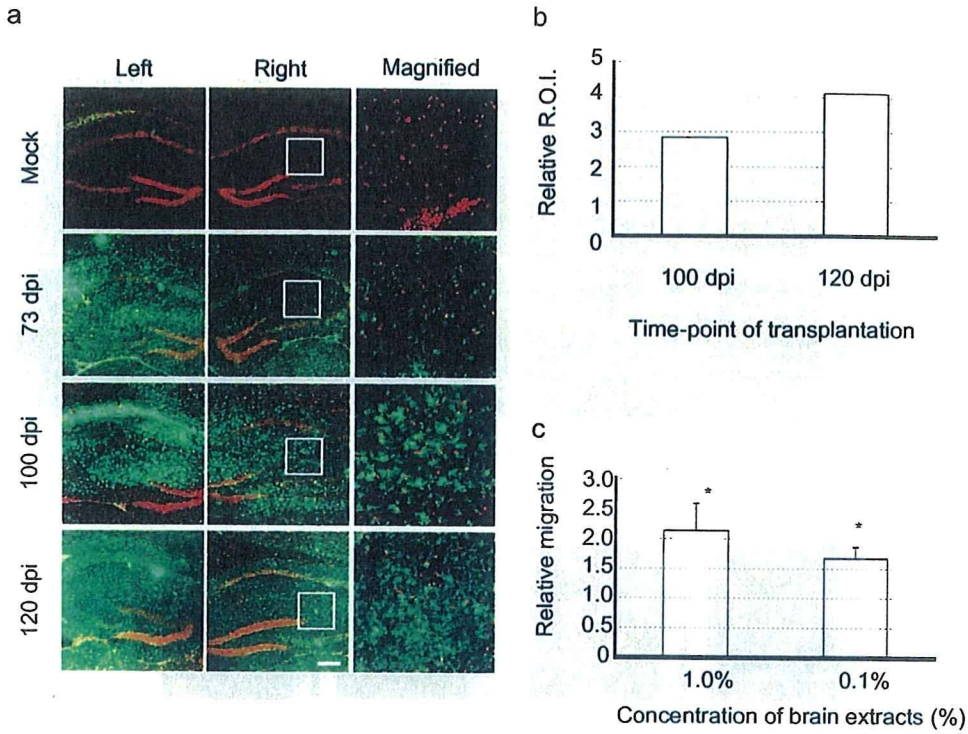

FIG. 2. Migration of hMSCs in response to prion-specific lesions. hMSCs (1×10^5 cells) were transplanted into the left hippocampi of mice infected with strain Chandler at 73, 100, or 120 dpi and into those of mock-infected mice at 120 dpi. One week after transplantation, the migration of hMSCs (green) to the contralateral hippocampus (right) was analyzed. The rightmost panels show magnified images of the regions boxed in the panels immediately to the left. Bar, 200 μm. (b) Quantification of hMSC migration. Areas positive for β-Gal in the contralateral hippocampus (regions of interest [ROI]) were measured using NIH Image J. The graph shows the levels of ROIs for mice transplanted at 100 and 120 dpi relative to that for a mouse transplanted at 73 dpi. (c) Migration of hMSCs to extracts from the brains of prion-infected mice. Insert wells containing an hMSC suspension were placed in the lower chambers, which contained 1.0 or 0.1% brain extract in serum-free DMEM, and were incubated for 24 h. The mean migration of hMSCs to brain extracts from mock-infected mice was arbitrarily set at 1, and the relative migration to brain extracts from mice infected with strain Chandler is indicated. Means and standard deviations from three independent assays (triplicate in each assay) are shown. *, $P < 0.05$.

eral hippocampus. In contrast, migration of hMSCs to the thalamus, where moderate PrP^{Sc} deposition had already occurred, was clearly observed (data not shown). In addition, more hMSCs were detected in the contralateral hippocampus when the transplantation was carried out at later time points (Fig. 2a). To compare the migration of hMSCs quantitatively, the total area of the hMSCs in the contralateral hippocampus (areas positive for β-Gal) was measured using the NIH Image J program. Compared to the migration of hMSCs to the contralateral hippocampus a week after the transplantation at 73 dpi, 2.8 and 4.1 times more hMSCs were detected when the transplantation was done at 100 and 120 dpi, respectively (Fig. 2b). We examined at least two mice from each experimental group and confirmed the consistency of the findings. Since PrP^{Sc} accumulation and astrocytosis in the hippocampi of mice infected with strain Chandler were first detected around 90 dpi and the levels of PrP^{Sc} accumulation and astrocytosis increased gradually thereafter (see Fig. S1 in the supplemental material), the migration of hMSCs to the contralateral hippocampus appeared to correlate with the severity of pathological changes.

Next, we analyzed the migration of hMSCs to brain extracts from prion-infected mice in vitro. Insert wells of a QCM 24-well colorimetric cell migration assay kit containing hMSCs were placed in the lower chambers, which contained 1.0 or 0.1% brain extract from prion- or mock-infected mice, and were incubated for 24 h. Cells that had migrated to the back sides (facing the lower chamber) of the membranes of the insert wells were quantified according to the supplier's instructions. Compared to the migration to brain extracts from mock-infected mice, approximately 2 and 1.5 times more hMSCs had migrated into the lower chambers containing 1.0% and 0.1% brain extracts from prion-infected mice, respectively (Fig. 2c). This suggests that chemoattractive factors that promote the migration of hMSCs are produced by the lesion caused by prion infection.

Migration of hMSCs into the brain after intravenous transplantation. MSCs have been reported to migrate to a site of brain injury even when they are introduced via intravenous injection (37, 38). To test if a similar phenomenon could be observed in prion-infected mice, hMSCs were intravenously inoculated into mice infected with strain Chandler or into mock-infected mice at 120 dpi. In mice infected with strain Chandler, hMSCs were observed in the hippocampus and thalamus even at 2 days after transplantation (data not shown). The cells showed a symmetrical distribution and appeared to increase in number in these tissues by 3 weeks posttransplantation (Fig. 3a; see also Fig. S2 in the supplemental material). In contrast, few MSCs were detected in the brains of mock-

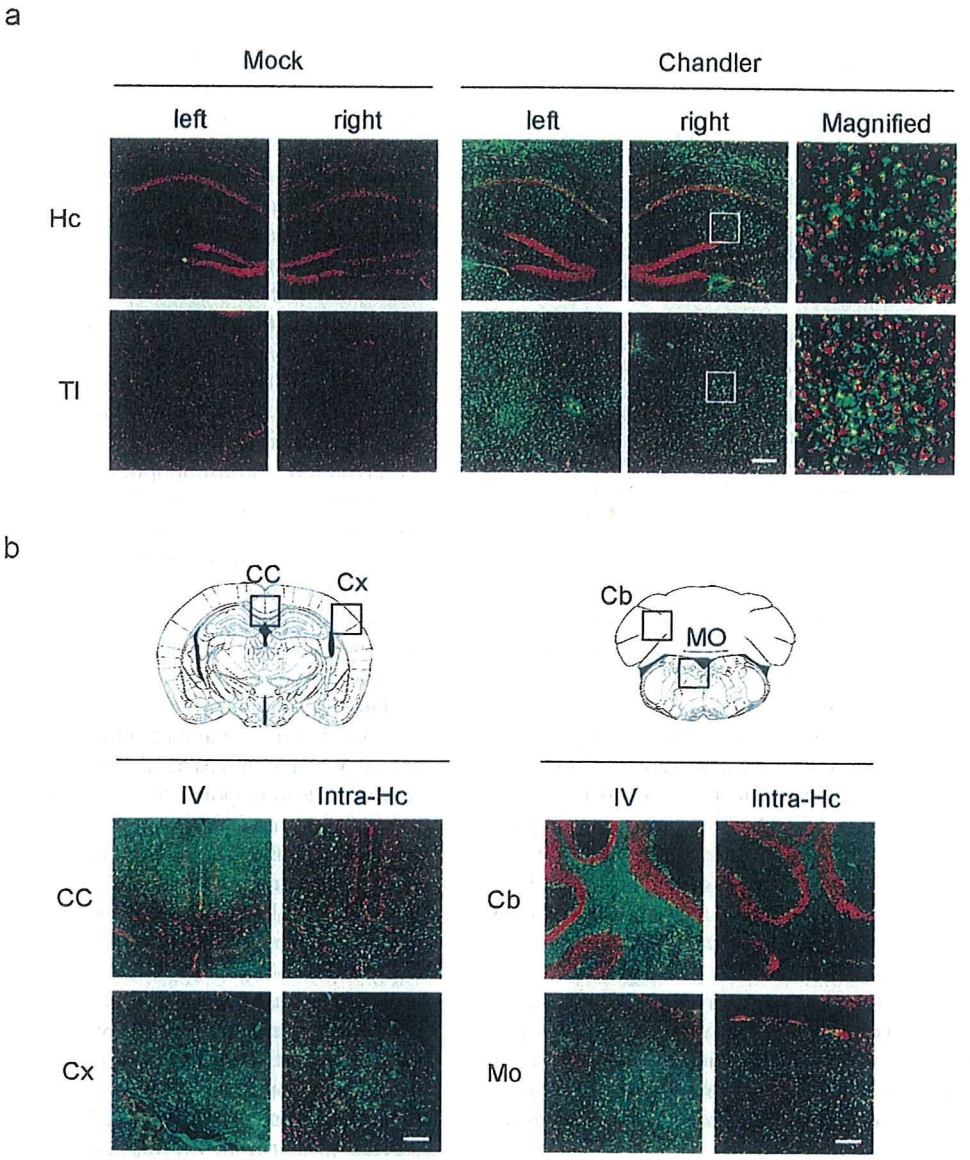

FIG. 3. Migration of hMSCs into the brain after intravenous transplantation. hMSCs (1×10^6 cells) were intravenously injected into mice infected with strain Chandler and into mock-infected mice at 120 dpi. Three weeks after injection, cryosections were prepared and stained with an anti-β-Gal MAb. (a) Presence of hMSCs in the left and right hippocampus (Hc) and thalamus (Tl) 3 weeks postinjection. The rightmost panels show magnified images of the regions boxed in the panels immediately to the left. Bar, 200 μm. (b) Distribution of hMSCs transplanted into the left hippocampus (Intra-Hc) or introduced via intravenous injection (IV). At 120 dpi, the hMSCs were transplanted into the left hippocampi (1×10^5 cells) or injected via the tail veins (1×10^6 cells) of mice infected with strain Chandler. The presence of hMSCs in the corpus callosum (CC), cortex (Cx), cerebellum (Cb), and medulla oblongata (MO) 3 weeks posttransplantation is shown. These brain regions are boxed on the images taken from Paxinos and Franklin and reprinted with permission of the publisher (39). Bars, 200 μm.

infected mice, demonstrating that the hMSCs migrated to the brain lesions caused by prion propagation. At each time point, we examined two mice for each experimental group and confirmed the consistency of the findings. The hMSCs were also well distributed in other brain regions, including the cerebral cortex, cerebellum, and medulla oblongata (Fig. 3b); however, consistent with the results shown in Fig. 3b, they did not migrate well to the hypothalamus (see Fig. S2 in the supplemental material). There was no difference in the area of hMSC distribution following intravenous versus intrahippocampal transplantation except at the corpus callosum. More hMSCs were observed in the corpus callosum after transplantation into the hippocampus than after intravenous injection, suggesting that cells migrate to the contralateral side through the corpus callosum after intrahippocampal transplantation (2).

Effects of transplantation of hMSCs on the survival of prion-infected mice. To examine whether the transplantation of hMSCs can ameliorate prion diseases, hMSCs were transplanted into the left hippocampi of mice infected with strain Chandler at 90 dpi. Figure 4 shows the survival curve for these mice. The intrahippocampal transplantation of hMSCs prolonged the survival of mice infected with strain Chandler

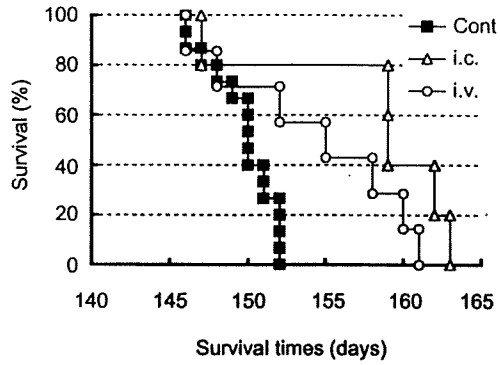

FIG. 4. Prolongation of survival of prion-infected mice by transplantation of hMSCs. For intracerebral (i.c.) transplantation, hMSCs (1×10^5 cells) were transplanted into the left hippocampi of mice infected with strain Chandler at 90 dpi ($n = 5$). For intravenous (i.v.) transplantation, 1×10^6 hMSCs were injected via the tail vein at 120 dpi ($n = 7$). The hMSC-transplanted and nontransplanted control (Cont) ($n = 15$) mice were observed until they reached the terminal stage of the disease. The graph shows survival curves.

(158 ± 6 days; $n = 5$) over that of the nontransplanted control group (150 ± 2 days; $n = 15$). Thus, hMSC transplantation prolonged mean survival by only 8 days, but this difference was statistically significant ($P < 0.01$ by the log rank test). We also transplanted hMSCs via the tail veins of mice infected with strain Chandler at 120 dpi. The transplantation of hMSCs via this peripheral route appeared not to be effective for nearly half of the mice; however, the remaining mice survived beyond the mean survival of the nontransplanted control group. Although the mean survival of hMSC-transplanted mice (154 ± 6 days; $n = 7$) was only a little longer than that of the control group, this difference was also significant ($P < 0.05$ by the log rank test). The fact that survival time was prolonged even when hMSCs were transplanted via a peripheral route after clinical onset (120 dpi) suggests that hMSCs have therapeutic potential for prion diseases. Since both intracerebral and intravenous transplantation of hMSCs prolonged the survival of prion-infected mice, we further analyzed the transplanted hMSCs.

Proliferation of hMSCs after transplantation. To examine the proliferation state of hMSCs that had migrated to lesions, BrdUrd was systemically administered after the transplantation of hMSCs to the left hippocampus. Three weeks posttransplantation, many BrdUrd-labeled nuclei were detected in the contralateral hippocampi and thalami of mice infected with strain Chandler (see Fig. S3 in the supplemental material), where many hMSCs had migrated (Fig. 1a). In contrast, few BrdUrd-labeled nuclei were detected in the contralateral hippocampi and thalami of mock-infected mice (see Fig. S3 in the supplemental material), although a few cells with BrdUrd-labeled nuclei were detected on the transplanted side (data not shown). BrdUrd-labeled cells were also observed in the cerebella and medullae oblongatae of mice infected with strain Chandler (data not shown). We examined two mice for each experimental group and confirmed the similar results. These results suggest that transplanted hMSCs are capable of proliferating in the microenvironment caused by prion propagation.

Expression of trophic factors in hMSCs. It is known that MSCs migrate to a site of injury in the brain and produce various trophic factors (8, 29). To ask if something similar happens in the case of prion disease, we next assayed the production of trophic factors in our model system. hMSCs were transplanted into the left thalamus at 120 dpi, and one mouse in each group was sacrificed and examined for the production of human trophic factors at 2 days and 1 and 3 weeks after transplantation. Immunoreactivities for human BDNF, NT3, and VEGF in the ipsilateral thalami of mice infected with strain Chandler became more intense from 2 days to 3 weeks posttransplantation. In contrast, no obvious increases, but rather decreases, in the signals of these trophic factors were observed for mock-infected mice (Fig. 5). Additionally, the expression of NGF, NT4/5, and CNTF was also upregulated (data not shown). These results suggest that hMSCs produce a variety of trophic factors in response to the neurodegeneration caused by prion infection.

Interestingly, only subpopulations of the hMSCs appeared to be positive for NT3 and BDNF. In addition, parts of the regions positive for these factors did not overlap with β-Gal staining. Since these antibodies are specific to human trophic factors and will not react with the corresponding mouse trophic factors, the presence of NT3 and BDNF in areas negative for β-Gal may represent trophic factors secreted from hMSCs and bound to mouse brain cells.

Differentiation of hMSCs. MSCs are known to differentiate into cells of neuronal and glial lineages in vivo and in vitro (11, 48, 61). We next asked if hMSCs differentiate into neuronal and glial cells in response to the lesions of prion diseases. At 3 weeks after transplantation into the thalamus, hMSCs positive for the neurodifferentiation marker MAP2, GFAP, or CNPase were detected in the brains of mice infected with strain Chandler (Fig. 6), although a relatively small number of hMSCs were positive for each marker. In contrast, no hMSCs positive for MAP2, GFAP, or CNPase were observed in the brains of mock-infected mice (data not shown), suggesting that neuronal and glial differentiation of hMSCs occurs in response to the neurodegeneration caused by prion infection. The GFAP-positive hMSCs were detected in the hippocampus, thalamus, and medulla oblongata. In contrast, MAP2-positive hMSCs were detected primarily in the hippocampus, cortex, and cerebellum, and CNPase-positive hMSCs were detected mainly in the cortex (data not shown).

DISCUSSION

The primary purpose of this study was to evaluate the potential of MSCs for treating prion diseases in a mouse model. For this purpose, the use of mouse MSCs would have been desirable; however, no appropriate method for the isolation of mouse MSCs from bone marrow had been established by the beginning of this study. On the other hand, it was well known that MSCs avoid allogeneic rejection (47). Thus, we adopted hMSCs to the mouse model and showed that hMSCs responded to the neuropathological lesions of prion diseases and may have therapeutic potential. Transplantation of MSCs is known to ameliorate neurological dysfunctions in experimental models (7, 23, 24, 30, 37). In clinical trials in which autologous MSCs are transplanted into patients with multiple system atrophy (28) or amyotrophic lateral sclerosis (33), or into patients who have suffered a stroke (3), there is some evidence of

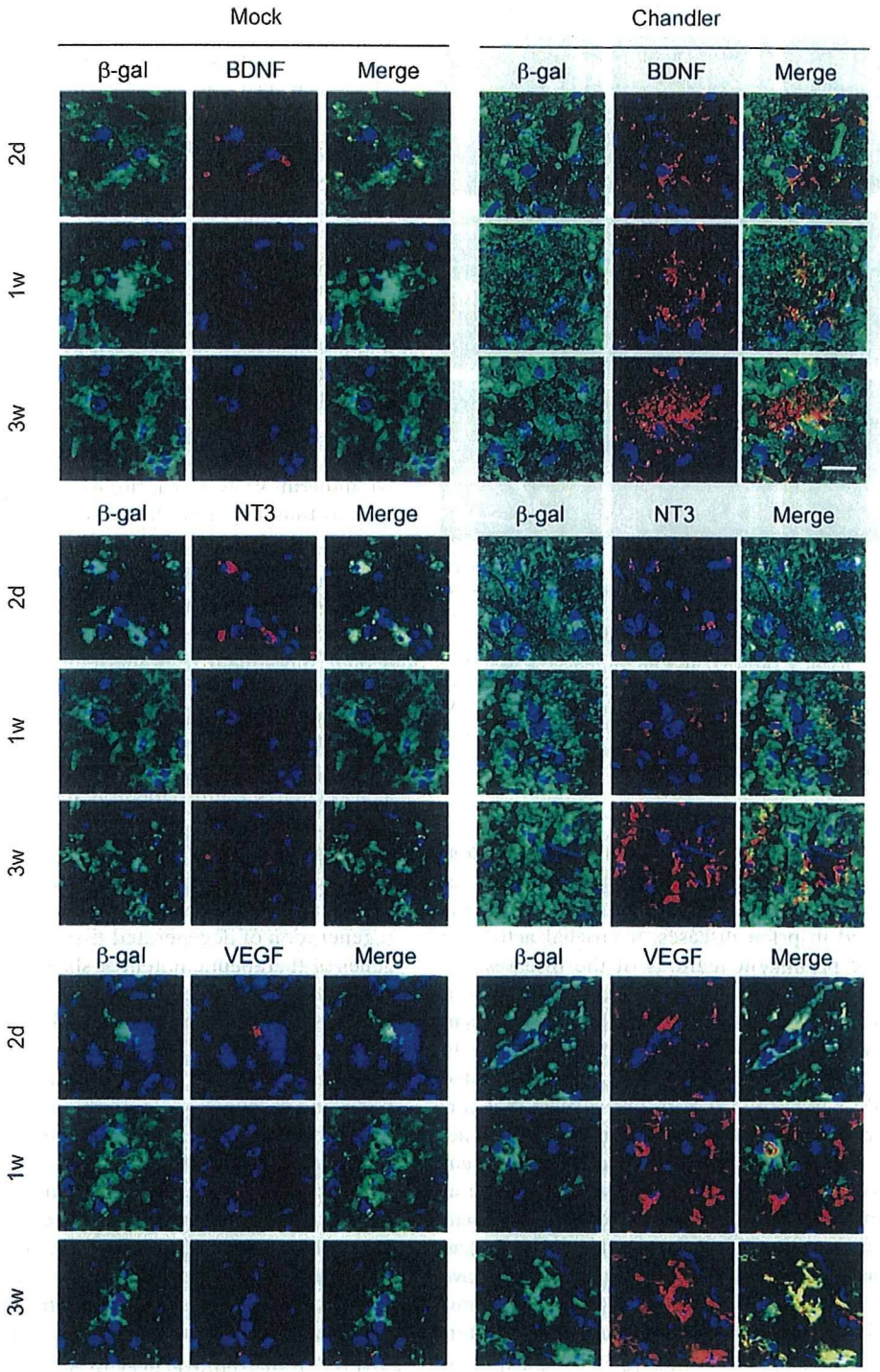

FIG. 5. Expression of trophic factors in hMSCs. hMSCs (1×10^5 cells) were transplanted into the left thalami of mice infected with strain Chandler and into those of mock-infected mice at 120 dpi. Two days (2d), 1 week (1w), and 3 weeks (3w) posttransplantation, cryosections were prepared and doubly stained with an anti-β-Gal MAb, for hMSCs (green), and an antibody against a human trophic factor (BDNF, NT3, or VEGF) (red). Nuclei were counterstained with DAPI (blue). Bar, 20 μm.

a beneficial effect without any adverse effects. How the introduction of MSCs leads to improved outcomes is not yet clear. However, the transplanted MSCs are known to migrate and home to a site of injury. Moreover, in this context, MSCs are expected to restore injured tissues by protecting neural tissues via secretion of various trophic factors (8), promotion of angiogenesis (20), stimulation of the proliferation and differentiation of endogenous neural stem cells (36), integration into tissues by differentiation or cell fusion (1), and modulation of the local immune response (64).

Here we showed that the level of migration of MSCs to the contralateral side of the mouse brain correlates with the de-

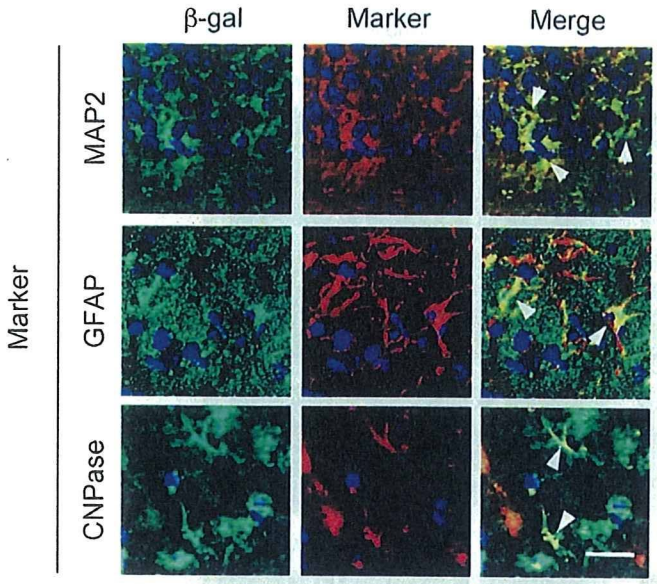

FIG. 6. Differentiation of hMSCs into cells of neuronal and glial lineages. At 120 dpi, hMSCs (1×10^5 cells) were transplanted into the left thalami of mice infected with strain Chandler. Three weeks post-transplantation, cryosections were prepared and doubly stained with an anti-β-Gal MAb, for hMSCs (green), and an antibody against a marker for neurons (MAP2), astrocytes (GFAP), or oligodendrocytes (CNPase) (red). Nuclei were counterstained with DAPI (blue). Arrows indicate hMSCs positive for each marker protein. The brain region for MAP2 and GFAP is the ipsilateral hippocampus, while that for CNPase is the cerebral cortex. Bar, 20 μm.

gree of PrP^{Sc} accumulation and the severity of histopathological changes in the prion-infected brain (Fig. 1d and 2). Although no antigen-specific humoral or cellular immune response is provoked in prion diseases, microglial activation and astrocytosis are prominent features of the diseases. Indeed, the expression of inflammatory cytokines and chemokines, which are likely to be produced in glial cells, is upregulated in the middle to late stage of prion infection (5, 6). In addition, brain extracts from prion-infected mice promoted chemotaxis of hMSCs in vitro. These results suggest that certain factors produced in the brains of prion-infected mice act as chemoattractive factors for hMSCs, although it is not clear whether the effects of mouse factors on human MSCs are as efficient as those on homologous MSCs. Monocyte chemoattractive protein 1 (known as CCL2), interleukin-8 (IL-8), and macrophage inflammatory protein 1α (known as CCL3) have been reported to enhance the migration of MSCs to ischemic brain tissue (57, 58). It was recently reported that an interaction between stromal cell-derived factor 1 (known as CXCL12), produced in ischemic brain lesions, and CXCR4, expressed on MSCs, plays an important role in the migration of MSCs (59). Because the inflammatory response and glial activation are common events in many neurological disorders, it is conceivable that a similar mechanism may account to some extent for the migration of MSCs to brain lesions associated with prion disease. For instance, we have found that the expression of CCL3 is upregulated in the thalami and medullae of prion-infected mice (unpublished observation). Experiments are under way to identify the chemoattractive factors by use of an in vitro chemotaxis assay.

MSCs have been reported to migrate to a site of brain injury even when intravenously injected (37, 38). Consistent with previous reports, our results showed here that hMSCs transplanted via intravenous injection travel to areas of brain lesions in prion-infected mice (Fig. 3). In prion diseases, although impairment of the blood-brain barrier (BBB) was observed in the cerebellum (56), no significant impairment of the BBB was observed in the hippocampus or cerebral cortex at the time of clinical onset or even at a later stage (42, 56). Thus, passive translocation of MSCs to the brain parenchyma through a disrupted BBB seems unlikely. Instead, active transendothelial migration of MSCs, similar to the recruitment of leukocytes and monocytes from the bloodstream to an inflammation site, is expected to be involved in the engraftment of MSCs transplanted via intravenous injection. Vascular cell adhesion molecule 1 and p-selectin expressed on the endothelium are important for the adhesion of MSCs to the endothelium via the β1 integrin VLA-4 (16, 46, 51). Proinflammatory cytokines, such as tumor necrosis factor alpha and IL-1β, upregulate the expression of adhesion molecules in endothelial cells (32). Indeed, tumor necrosis factor alpha and IL-1β are upregulated during the course of prion disease (6, 49), suggesting that these cytokines induce the adherence of MSCs to the endothelium and their subsequent transendothelial migration to the brain lesions. Understanding how the migration of MSCs to brain lesions affected by prion diseases is regulated, and further elucidation of the mechanisms underlying the tropism of MSCs, may provide new insight into the engraftment of MSCs as it relates to the progression and possible treatment of neurodegenerative diseases.

The ability of MSCs to migrate to a site of injury has been given particular attention, because it suggests that these cells can act as a vehicle for gene therapy in addition to aiding in the regeneration of degenerated tissues. Indeed, MSCs expressing genes of therapeutic potential showed a greater positive effect on functional recovery than unmodified MSCs (24, 37, 38). Transgenic expression of anti-PrP antibodies (22), a fusion protein between PrP^C and the Fc portion of immunoglobulin (PrP-Fc) (34), and dominant-negative PrP mutants (40) inhibited prion propagation. In addition, expression of anti-PrP Fab fragments and PrP-Fc in the brain by virus vectors has been reported to antagonize prion propagation in the brain (18, 62). Furthermore, intraventricular infusion of an anti-PrP MAb slowed the formation of neuropathological lesions and prolonged the survival of prion-infected mice even when the MAb was administered at clinical onset (53). However, large macromolecules, such as immunoglobulins, are expected to be delivered to the lesions inefficiently. Indeed, the distribution of MAbs was restricted primarily to the hippocampus and thalamus, even when the MAbs were infused directly into the lateral ventricle (53). Therefore, the observation that hMSCs target and home to brain lesions associated with prion diseases indicates the potential utility of hMSCs as a cellular vehicle for the delivery of therapeutic genes to brain lesions.

We showed here that microenvironments in the brain lesions associated with prion disease stimulate MSCs to produce various trophic factors: BDNF, NGF, VEGF, and others. These trophic factors are reported to have antiapoptotic effects, to promote nerve fiber regeneration, and to induce endogenous cell proliferation and angiogenesis in injured brains (9, 29, 31).

It remains to be elucidated whether the prolonged survival of prion-infected mice by hMSC transplantation can be attributed to the secretion of trophic factors from hMSCs. Although hMSCs alone may have the ameliorative effect to some extent, they could not arrest the disease progression caused by prion propagation. Similarly, it has been shown that antagonizing prion propagation can slow disease progression but cannot ameliorate functional deficits (13, 25, 53). Thus, it seems possible that the combination of MSCs with inhibitors of prion propagation would have a synergistic effect in the treatment of prion diseases.

Replacement of damaged neurons with differentiated MSCs or their fusion with MSCs after MSC transplantation is an attractive possible route to the restoration of neurological functions (11, 54, 60). In this study, we showed that small populations of MSCs were differentiated into cells expressing neuronal, astrocyte, or oligodendrocyte markers. Because only a small portion of transplanted MSCs differentiated into a neuronal and a glial lineage in vivo, it seems unlikely that the prolongation of survival could be attributed directly to differentiation. However, induction of neuronal differentiation in vitro prior to transplantation improves functional outcomes in a rat model of Parkinson's disease and cerebral infarction (12, 35). Therefore, appropriate preconditioning may enhance the effects of *trans*-differentiation on the restoration of degenerated tissues.

To our knowledge, this is the first report showing the therapeutic potential of MSCs for prion diseases. We showed that hMSCs home to the lesions, produce trophic factors, and differentiate into neuronal and glial lineage cells in response to the microenvironment in the lesions. As we are already aware, not only inhibition of prion propagation but also regeneration of damaged nervous tissues is required for recovery from prion diseases. Thus, a combination of genes possessing antiprion effects with MSCs, which can deliver therapeutic genes and have potential for neuroprotection and the regeneration of damaged tissues, may provide an effective treatment for prion diseases.

ACKNOWLEDGMENTS

This work was supported by the Regional New Consortium R&D Projects of the Ministry of Economy, Trade and Industry of Japan; by a grant from the global COE Program (F-001), a Grant-in-Aid for Science Research (A) (grant 18208026), and a Grant-in-Aid for Exploratory Research (grant 20658070) from the Ministry of Education, Culture, Sports, Science, and Technology of Japan; and by a grant from the Ministry of Health, Labor and Welfare of Japan (grant 20330701). This work was also partly supported by a grant for Strategic Cooperation to Control Emerging and Reemerging Infections and by the Program of Founding Research Centers for Emerging and Reemerging Infectious Diseases, from the Ministry of Education, Culture, Sports, Science, and Technology of Japan.

REFERENCES

1. **Alvarez-Dolado, M., R. Pardal, J. M. Garcia-Verdugo, J. R. Fike, H. O. Lee, K. Pfeffer, C. Lois, S. J. Morrison, and A. Alvarez-Buylla.** 2003. Fusion of bone-marrow-derived cells with Purkinje neurons, cardiomyocytes and hepatocytes. Nature **425**:968–973.
2. **Azizi, S. A., D. Stokes, B. J. Augelli, C. DiGirolamo, and D. J. Prockop.** 1998. Engraftment and migration of human bone marrow stromal cells implanted in the brains of albino rats—similarities to astrocyte grafts. Proc. Natl. Acad. Sci. USA **95**:3908–3913.
3. **Bang, O. Y., J. S. Lee, P. H. Lee, and G. Lee.** 2005. Autologous mesenchymal stem cell transplantation in stroke patients. Ann. Neurol. **57**:874–882.
4. **Bone, I., L. Belton, A. S. Walker, and J. Darbyshire.** 2008. Intraventricular pentosan polysulphate in human prion diseases: an observational study in the UK. Eur. J. Neurol. **15**:458–464.
5. **Burwinkel, M., C. Riemer, A. Schwarz, J. Schultz, S. Neidhold, T. Bamme, and M. Baier.** 2004. Role of cytokines and chemokines in prion infections of the central nervous system. Int. J. Dev. Neurosci. **22**:497–505.
6. **Campbell, I. L., M. Eddleston, P. Kemper, M. B. Oldstone, and M. V. Hobbs.** 1994. Activation of cerebral cytokine gene expression and its correlation with onset of reactive astrocyte and acute-phase response gene expression in scrapie. J. Virol. **68**:2383–2387.
7. **Chen, J., Y. Li, L. Wang, M. Lu, X. Zhang, and M. Chopp.** 2001. Therapeutic benefit of intracerebral transplantation of bone marrow stromal cells after cerebral ischemia in rats. J. Neurol. Sci. **189**:49–57.
8. **Chopp, M., and Y. Li.** 2002. Treatment of neural injury with marrow stromal cells. Lancet Neurol. **1**:92–100.
9. **Crigler, L., R. C. Robey, A. Asawachaicharn, D. Gaupp, and D. G. Phinney.** 2006. Human mesenchymal stem cell subpopulations express a variety of neuro-regulatory molecules and promote neuronal cell survival and neuritogenesis. Exp. Neurol. **198**:54–64.
10. **Demaimay, R., K. T. Adjou, V. Beringue, S. Demart, C. I. Lasmézas, J. P. Deslys, M. Seman, and D. Dormont.** 1997. Late treatment with polyene antibiotics can prolong the survival time of scrapie-infected animals. J. Virol. **71**:9685–9689.
11. **Deng, J., B. E. Petersen, D. A. Steindler, M. L. Jorgensen, and E. D. Laywell.** 2006. Mesenchymal stem cells spontaneously express neural proteins in culture and are neurogenic after transplantation. Stem Cells **24**:1054–1064.
12. **Dezawa, M., H. Kanno, M. Hoshino, H. Cho, N. Matsumoto, Y. Itokazu, N. Tajima, H. Yamada, H. Sawada, H. Ishikawa, T. Mimura, M. Kitada, Y. Suzuki, and C. Ide.** 2004. Specific induction of neuronal cells from bone marrow stromal cells and application for autologous transplantation. J. Clin. Investig. **113**:1701–1710.
13. **Doh-ura, K., K. Ishikawa, I. Murakami-Kubo, K. Sasaki, S. Mohri, R. Race, and T. Iwaki.** 2004. Treatment of transmissible spongiform encephalopathy by intraventricular drug infusion in animal models. J. Virol. **78**:4999–5006.
14. **Farquhar, C. F., and A. G. Dickinson.** 1986. Prolongation of scrapie incubation period by an injection of dextran sulphate 500 within the month before or after infection. J. Gen. Virol. **67**:463–473.
15. **Ferrari, G., G. Cusella-De Angelis, M. Coletta, E. Paolucci, A. Stornaiuolo, G. Cossu, and F. Mavilio.** 1998. Muscle regeneration by bone marrow-derived myogenic progenitors. Science **279**:1528–1530.
16. **Fox, J. M., G. Chamberlain, B. A. Ashton, and J. Middleton.** 2007. Recent advances into the understanding of mesenchymal stem cell trafficking. Br. J. Haematol. **137**:491–502.
17. **Furuoka, H., A. Yabuzoe, M. Horiuchi, Y. Tagawa, T. Yokoyama, Y. Yamakawa, M. Shinagawa, and T. Sata.** 2005. Effective antigen-retrieval method for immunohistochemical detection of abnormal isoform of prion proteins in animals. Acta Neuropathol. **109**:263–271.
18. **Genoud, N., D. Ott, N. Braun, M. Prinz, P. Schwarz, U. Suter, D. Trono, and A. Aguzzi.** 2008. Antiprion prophylaxis by gene transfer of a soluble prion antagonist. Am. J. Pathol. **172**:1287–1296.
19. **Goñi, F., E. Knudsen, F. Schreiber, H. Scholtzova, J. Pankiewicz, R. Carp, H. C. Meeker, R. Rubenstein, D. R. Brown, M. S. Sy, J. A. Chabalgoity, E. M. Sigurdsson, and T. Wisniewski.** 2005. Mucosal vaccination delays or prevents prion infection via an oral route. Neuroscience **133**:413–421.
20. **Hamano, K., T. S. Li, T. Kobayashi, S. Kobayashi, M. Matsuzaki, and K. Esato.** 2000. Angiogenesis induced by the implantation of self-bone marrow cells: a new material for therapeutic angiogenesis. Cell Transplant. **9**:439–443.
21. **Hellmann, M. A., H. Panet, Y. Barhum, E. Melamed, and D. Offen.** 2006. Increased survival and migration of engrafted mesenchymal bone marrow stem cells in 6-hydroxydopamine-lesioned rodents. Neurosci. Lett. **395**:124–128.
22. **Heppner, F. L., C. Musahl, I. Arrighi, M. A. Klein, T. Rülicke, B. Oesch, R. M. Zinkernagel, U. Kalinke, and A. Aguzzi.** 2001. Prevention of scrapie pathogenesis by transgenic expression of anti-prion protein antibodies. Science **294**:178–182.
23. **Hofstetter, C. P., E. J. Schwarz, D. Hess, J. Widenfalk, A. El Manira, D. J. Prockop, and L. Olson.** 2002. Marrow stromal cells form guiding strands in the injured spinal cord and promote recovery. Proc. Natl. Acad. Sci. USA **99**:2199–2204.
24. **Jin, H. K., J. E. Carter, G. W. Huntley, and E. H. Schuchman.** 2002. Intracerebral transplantation of mesenchymal stem cells into acid sphingomyelinase-deficient mice delays the onset of neurological abnormalities and extends their life span. J. Clin. Investig. **109**:1183–1191.
25. **Kawasaki, Y., K. Kawagoe, C. J. Chen, K. Teruya, Y. Sakasegawa, and K. Doh-ura.** 2007. Orally administered amyloidophilic compound is effective in prolonging the incubation periods of animals cerebrally infected with prion diseases in a prion strain-dependent manner. J. Virol. **81**:12889–12898.
26. **Kobune, M., Y. Kawano, Y. Ito, H. Chiba, K. Nakamura, H. Tsuda, K. Sasaki, H. Dehari, H. Uchida, O. Honmou, S. Takahashi, A. Bizen, R. Takimoto, T. Matsunaga, J. Kato, K. Kato, K. Houkin, Y. Niitsu, and H. Hamada.** 2003. Telomerized human multipotent mesenchymal cells can dif-